Spatial Organization of Large Cells

A dissertation presented

by

Martin Helmut Wuehr

to

The Committee on Higher Degrees in Systems Biology

in partial fulfillment of the requirements
for the degree of
Doctor of Philosophy in the subject of
Systems Biology

Harvard University
Cambridge, Massachusetts

March 2010

Timothy John Mitchison Martin Helmut Wuehr

Spatial Organization of Large Cells

Abstract

The rationale for my research was to investigate unusually large cells, fertilized frog and fish eggs, to obtain a unique perspective on a cell's spatial organization with a focus on cell division.

First, we investigated how spindle size changes during cleavage stages while cell size changes by orders of magnitude. To do so we improved techniques for immunofluorescence in amphibian embryos and generated a transgenic fish line with fluorescently labeled microtubules. We show that in smaller cells spindle length scales with cell length, but in very large cells spindle length approaches an upper limit and seems uncoupled from cell size. Furthermore, we were able to assemble mitotic spindles in embryonic extract that had similar size as in vivo spindles. This indicates that spindle size is set by a mechanism that is intrinsic to the spindle and not downstream of cell size.

Second we investigated how relatively small spindles in large cells are positioned, and oriented for symmetric cell division. We show that the localization and orientation of these spindles are determined by location and

orientation of sister centrosomes set by the anaphase-telophase aster of the previous cycle.

Third we researched the mechanism by which asters center and align centrosomes relative to the longest axis. With a novel light-activated drug we could asymmetrically perturb asters. The asters moved away from the site of perturbation indicating that asters are positioned with pulling and not pushing forces. We show that the pulling forces are dynein dependent and act before astral microtubules contact the cortex they are moving toward, so dynein must pull on bulk cytoplasm, not the cell cortex as usually proposed. The cortex acts to limit microtubule length, which indirectly controls the strength of dynein-dependent pulling forces, and thus centers the aster in the cell. Where two sister asters overlap a microtubules sparse region we call "exclusion zone" emerges. This zone limits microtubule length, and thus promotes outward movement of sister asters

We present a model in which dynein pulling on bulk cytoplasm, operating in conjunction with microtubule-length limiting mechanisms, centers nascent spindles, and orient them along the long axis of the cell. This model explains cleavage plane geometry in early vertebrate embryos, and may apply more generally.

Table of Content

A transparent egg as it develops is one of the most fascinating objects in the world of living beings. The continuous change in form that takes place from hour to hour puzzles us by its very simplicity. The geometric patterns that present themselves at every turn inivite mathematical analyses. The constancy and orderliness of the whole series of events, repeating themselves a thousendfold in every batch of eggs, assures us of a causal sequence conspiring to create an object whose parts are adjusted to make a machine of extraordinary complexity. (Morgan, 1927)

I. Background and Summary

Background

Amphibian and fish embryos are classical research models

Fertilization and development of fish was first described by Aristotle: “When the female has laid her eggs, the male sprinkles the milt over them and those eggs are fertilized which it reaches, but not the others; this shows that the male does not contribute anything to the quantity but only to the quality of the embryo.” (Aristotle, 350 BC). Around 1665 the Dutch biologist Swammerdam was probably the first person ever to witness cell division when he observed the two cell stage of a frog embryo: "Next I observed the whole of the little frog divided, as it were, into two parts by a very obvious fold or furrow." (Baker, 1951; Swammerdam, 1737) (Fig 1A).

It took until the early 19th century for researchers to rediscover the cleavage stage of amphibian embryos (J.L. Prevost, 1824; Rusconi, 1826) (Fig 1B). The first description of cleavage stages in fish embryos followed soon thereafter (Rusconi, 1836) (Fig 1C).

In this thesis I investigate the intracellular reorganizations that determine the well conserved cleavage planes in frog and fish embryos. I propose a model that

explains how these very large cells divide perpendicular to their longest axis, into two equally sized daughter cells.

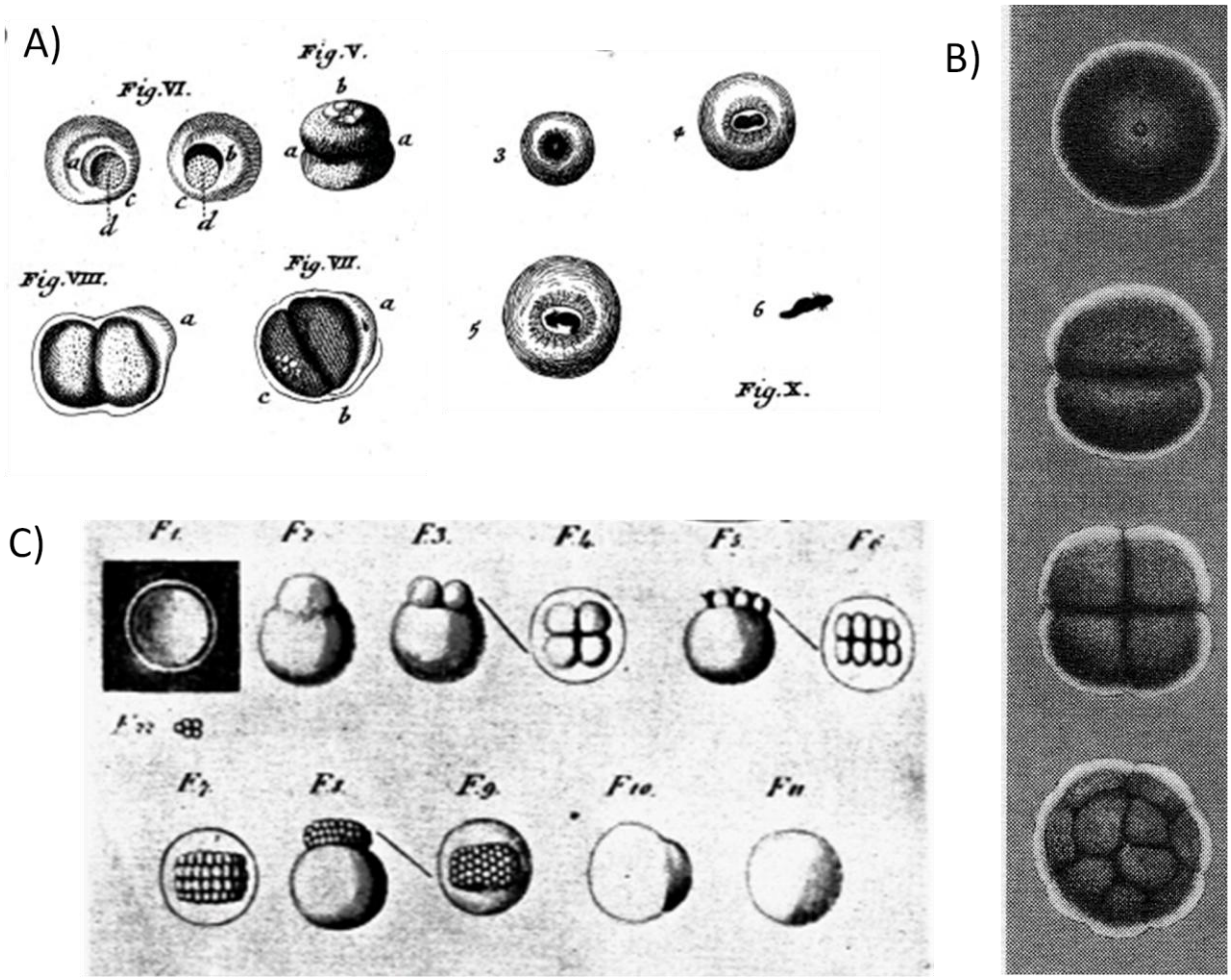

Figure I-1: Early drawing of amphibian and fish embryos at cleavage stage: A) reprint from Swammerdam's Biblia naturae. Depicting various stages of frog development including the two cell stage (Swammerdam, 1737) B) Rusconi's drawings of a salamander embryos and C) fish embryos at cleavage stage (Rusconi, 1826, 1836).

Intracellular reorganization during division

For the investigation of intracellular reorganization early amphibians embryos are far from optimal. Due to the high yolk content imaging is very difficult and required sectioning (Schultze, 1887) (Fig. 2 C). More recently imaging was improved by optical sectioning with confocal microscopes and incubation of fixed embryos in Murray's clear (Becker and Gard, 2006; Dent et al., 1989). This clear has a similar refractive index as yolk making the embryos transparent. However, even today imaging inside large amphibian cells is a major challenge.

In fish embryos yolk and cytoplasm are separated, cells are transparent. But for reasons that are not clear to me, fish embryos only very recently became a main-stream research model. Historically other transparent cells e.g. from salamander tissue or echinoderms provided initial clues how the cell's interior is (re)organized during cell division. With precursers of immunofluorescence, researchers like Flemming observed asters, the mitotic spindle and the separation of sister chromatids (Flemming, 1882) (Fig 2 A,B). This thesis focuses on the role of the asters, which are arrays of microtubules emanating from centrosomes.

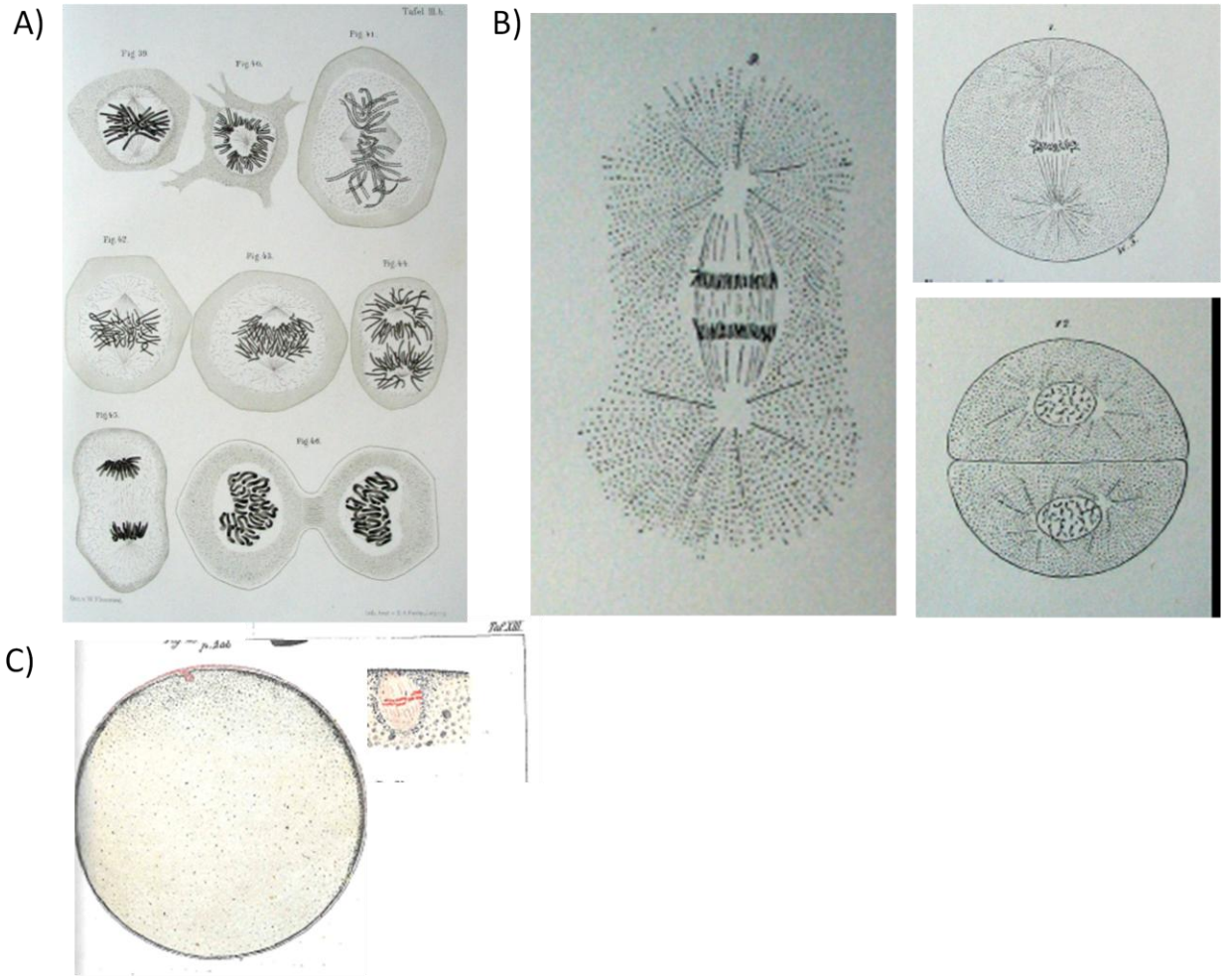

Figure I-2: Intracellular (re)organization of cell division A) Drawings of Flemming of various cell cycle stages of salamander tissue cells and B) sea urchin embryos (Flemming, 1882). C) The meiotic spindle of a frog egg by Schultze obtained by sectioning (Schultze, 1887)

The aster's functions in organizing the cell

For experiments in which observation from outside is sufficient, the early amphibian cell's robustness and large size provided researchers with unique experimental advantages: Hertwig and Pflüger elongated fertilized frog eggs by compression and observed that the cleavage plane reoriented perpendicular to

the cell's longest axis (Hertwig, 1893; Pflueger, 1884) (Fig 3 A). By combining this observation with knowledge of internal organization of transparent cells Hertwig proposed that the mitotic spindle aligns with the longest axis of the cell, determining the orientation of the cleavage plane (Hertwig, 1893) - a concept now known as Hertwig's rule. The alignment of the spindle with the cells' longest axis is believed to occur via interactions of the spindle's aster and the cortex (Bjerknes, 1986).

In interphase, asters are also critical for the cell's spatial organization: Relatively early it was observed that male and female nucleus follow the aster's rays to the center of the cell (Chambers, 1939). More recently this movement has been shown to be dynein dependent (Reinsch and Karsenti, 1997). In smaller tissue culture cells the interphase asters position centrosomes and the nucleus at the center of the cell (Burakov et al., 2003).

Another role of asters has been demonstrated by Rappaport. Through elegant manipulation of sand dollar embryos he was able to generate an aster-aster overlap from asters of two different spindles. This astral microtubule overlap was sufficient to induce an additional cleavage furrow (Rappaport, 1961) (Fig 3 B).

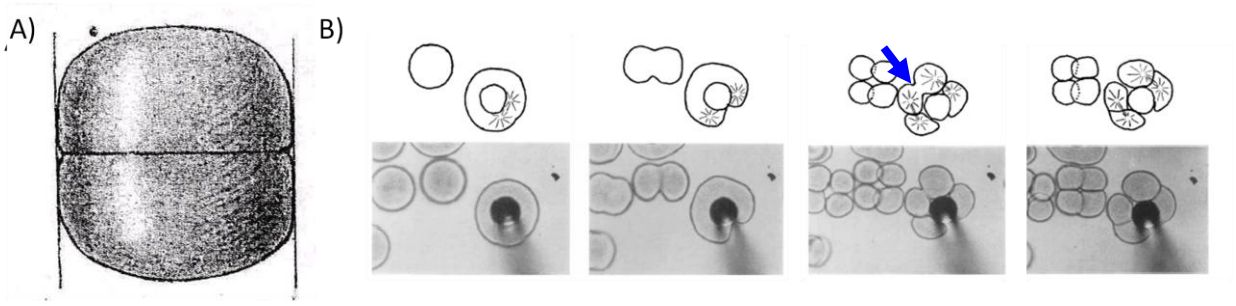

Figure I-3: The aster's role in organizing the cell A) Experiment by Hertwig in which he artificially elongated a fertilized frog egg and was able to reorient the first cleavage plane (Hertwig, 1893). Hertwig's rule proposes that the mitotic spindle aligns, supposedly with its aster along the longest axis of the cell determining the orientation of cleavage plane. B) By introducing a glass rod into the one cell stage of a sand dollar embryo Rappaport was able to generate an aster-aster overlap between two spindles. This led to the formation of an additional cleavage furrow (blue arrow) (Rappaport, 1961). (Reprinted with friendly permission from John Wiley and Sons).

How do asters position?

Aster positioning is clearly very important for the spatial organization of cells. But how does an aster find the correct position taking into account cellular shape and other asters?

A first explanation was proposed by Morgan "The movements of the asters [ ] become explicable on the view that the growing (polyspermic)-asters are more solid spheres floating in a more fluid medium. As they grow they push each other apart, and come to occupy positions in respect to each other that semi-solid bodies would assume in a more fluid sphere"(Morgan, 1927). Importantly at this time it was not yet clear what the aster's "rays" or "fibrilae" observed with primitive stains were. In the1950s and 60s various researchers observed straight rods with defined diameter (Palay, 1956). Slautterback, Ledbetter and Porter unified these findings and gave the structures the name microtubules (Ledbetter

and Porter, 1963; Slautterback, 1963). Soon thereafter Borisy and Taylor identified colchine-binding protein (tubulin) as the major component of the mitotic spindle (Borisy and Taylor, 1967). With the discovery of dynamic instability (Mitchison and Kirschner, 1984) and the deduction that microtubules growing into an obstacle can produce pushing forces (Hill and Kirschner, 1982). Morgan's pushing model got a molecular basis.

Evidence against pushing forces for aster centering came from beautiful experiments performed by Hamaguchi and Hiramotu (Hamaguchi and Hiramoto, 1986) (Fig 4). They incubated fertilized sand dollar eggs in the microtubule depolymerizer colcemid, which is light sensitive. By shining UV-light at a defined region they generated zones in which microtubules were allowed to grow. Interestingly, the sperm aster centered within a circle of UV-light and followed the circle's movements. Hamaguchi and Hiramotu interpreted this that the microtubules of the sperm aster would exert length dependent pulling forces. More recently it was discovered that microtubules, due to buckling, probably cannot transfer relevant pushing forces in cells larger than yeast (Dogterom et al., 2005; Faivre-Moskalenko and Dogterom, 2002). Localized perturbation of asters in interphase tissue culture cells and laser ablation in *C. elegans* confirmed that microtubules exert pulling forces in these cells (Burakov et al., 2003; Grill et al., 2003). In the asymmetric systems of budding yeast and *C. elegans* microtubules are believed to pull from the cortex (Grill et al., 2003; Lee et al., 2000). For reasons that are not entirely clear to me the current canonical

model on how asters center is that they pull on the cellular cortex (Dogterom et al., 2005; Kunda and Baum, 2009). The simplest form of this model would not lead to centering but to movement of the aster into the cortex. To generate a force towards the cell's center Hyman and Grill suggested that the number of pulling sites would be limited relative to the number of microtubules touching the cortex (Grill and Hyman, 2005). This is supported by experimental evidence that in *C. elegans* the amount of force generators is limited compared to the number of microtubules (Grill et al., 2003).

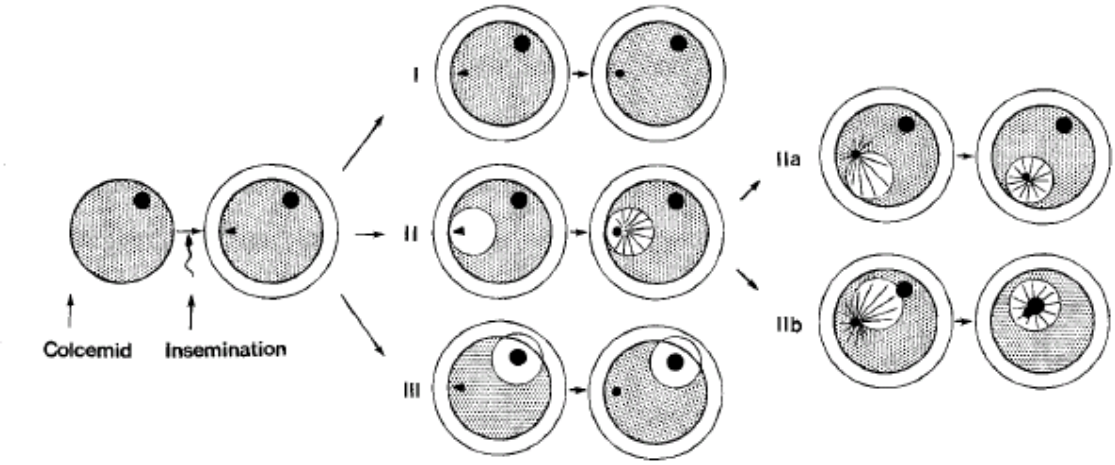

Figure I-4: Hamaguchi and Hiramoto incubated fertilized sand dollar embryos in light sensitive Colcemid. By UV-irradiation (white circle) they could generate a zone that allowed microtubules growth. The sperm aster centered in that zone and followed it when moved. Black circle represents female nucleus, triangle represents centrosome (Hamaguchi and Hiramoto, 1986). (Reprinted with friendly permission from John Wiley and Sons)

In summary, how cells determine the geometry for cell division is poorly understood on any scale. Interpretations of different experiments from different systems are conflicting. For the large amphibian and fish cells an additional burden was that only very few micrographs depicting internal organization were published.

Summary of thesis

Chapter II (published in Current Biology, 2008)

Cell length in amphibian embryos during cleavage stage changes by orders of magnitude within a few hours. We wondered if, and how, mitotic spindle length adapts to function at these different length scales. To investigate microtubule-organization during the cleavage stages in the frog *Xenopus laevis* we improved immunofluorescence methods by changing fixation conditions to allow faster and deeper antibody penetration. This reduced incubation time from two weeks to two days and avoided time consuming sectioning.

We were able to follow spindle length systematically during early development. We show that spindle length increases with cell length in small cells, but in cells larger than ~200 µm up to ~1200 µm spindle length approaches an upper limit of ~60 µm. Furthermore, we were able to make extract from fertilized embryos that formed spindles of similar size in vitro, indicating that spindle size is set by an intrinsic mechanism and not simply downstream of cell-size.

We were surprised to see the very small spindle of the early stages in a much larger cell, centered and aligned with the cell's longest axis. How could this be accomplished? The astral microtubules seemed to be far too short to sense cellular shape.

We show that the location of the spindles is set by the anaphase-telophase aster of the previous cell cycle. These asters are large enough to sense cellular shape and locate the centrosomes and DNA at the center of the cell. Once the cell cycle

enters mitosis the anaphase-telophase aster breaks down and the tiny metaphase spindle forms at the location where DNA and centrosomes were deposited. For the first mitotic spindle the sperm-aster fulfills this task. Having observed how location is determined for the metaphase spindle we hypothesized that the aster of the previous cell cycle also determines the metaphase-spindle's orientation along the longest cell axis. We confirmed this hypothesis in chapter IV.

Chapter III (Published in Cell Cycle, 2009)

Telophase and sperm aster's placement of centrosomes and DNA determine localization of the mitotic spindles and therefore ultimately localization of the cleavage plane. In chapter III we compare models for aster centering proposed for smaller cells with our acquired knowledge of microtubules organization in early frog embryos.

We could rule out the current canonical centering model, in which astral microtubules pull from the cortex. This model is inconsistent with observations in amphibian embryos in which asters move without touching the cortex in the direction of movement and the ability of multiple asters in a polyspermic embryo to space out relative to each other (Herlant, 1911).

At this point we could not distinguish between a scenario where asters would center by pushing against the cellular boundary (Morgan, 1927) or a scenario where microtubules would be pulled on along their sides (Hamaguchi and Hiramoto, 1986) (e.g. by minus end directed motors anchored in cytoplasm). Back of the envelope calculations with plausible scenarios, like crosslinking or

lateral enforcement, are consistent with microtubules being able to transfer relevant pushing forces over millimeter distance. In chapter IV we performed experiments that were able to distinguish between these models.

In chapter III we also describe a microtubules free zone that emerges where two asters touch each other. We discuss possible mechanism how this “exclusion zone” could be generated. We believe that this zone allows asters to recognize each other and provides the information for the telophase asters to move from the center of the mother cell to the two centers of the future daughter cells. In the “pulling on cytoplasm” model the interaction zone would provide the asymmetry of the aster necessary to provide net forces. In the case of the pushing model the interaction zone would provide the barrier microtubules could push against.

Chapter IV (paper in preparation)

In chapter IV we test the hypotheses proposed in chapters II and III on how large cells determine their center and longest axis.

A major drawback of experiments in amphibian embryos is that live imaging deep inside the cells is impossible. Immunofluorescence of early fish and frog embryos indicated that microtubules organization in both is very similar but in fish live imaging is possible. We therefore generated a transgenic zebrafish expressing the microtubule binding part of ensconsin labeled with GFP (EMTB-3xGFP). We observed that in fish, like in frog, the asters move without touching the cortex. To distinguish between pushing and pulling models of chapter III for centering we

developed a caged form of the microtubules depolymerizer Combretastatin 4A. This allowed us to perturb microtubule dynamics in a temporally and spatially defined manner. When we uncaged the drug next to an aster, the aster disassembled asymmetrically and moved away from the site of perturbation arguing for pulling and against pushing forces. The asters lost their ability to move centrosomes in frog and fish upon injection of the dynactin inhibitor p150-CC1, suggesting that dynein generates the pulling forces for centering. Also in frog embryos the sperm aster's movement was inhibited upon p150-CC1 injection.

Having learned more about how large cells determine their center we next focused on how they would determine their longest axis. Upon squishing between glass plates at the one cell stage we observed that the centrosomes realigned with the artificial longest axis before nuclear envelope breakdown. This confirms the hypothesis from chapter II that the aster of the previous cycle determines the orientation of the metaphase spindle. We furthermore show that the orientation of duplicated-centrosomes within an aster is not dependent on aster cortex contact, but alignment with the longest axis of the aster is lost upon inhibition of dynein.

For the first time we can posit a unified model that explains centering and longest axis determination for during the cleavage stages of early amphibian and fish embryos. This model depends on dynein pulling from bulk cytoplasm, and microtubule length limitation by the cortex and by aster-aster interactions. Our

model finds strong support in very large cells, but it might apply more generally, to any system where asters or spindles center by pulling forces.

References

Aristotle (350 BC). On the generation of animals. *I.730a20, translated by Arthur Platt*.

Baker, J.R. (1951). Remarks on the discovery of cell-division. Isis *42*, 285-287.

Becker, B.E., and Gard, D.L. (2006). Visualization of the cytoskeleton in Xenopus oocytes and eggs by confocal immunofluorescence microscopy. Methods Mol Biol *322*, 69-86.

Bjerknes, M. (1986). Physical theory of the orientation of astral mitotic spindles. Science *234*, 1413-1416.

Borisy, G.G., and Taylor, E.W. (1967). The mechanism of action of colchicine. Colchicine binding to sea urchin eggs and the mitotic apparatus. J Cell Biol *34*, 535-548.

Burakov, A., Nadezhdina, E., Slepchenko, B., and Rodionov, V. (2003). Centrosome positioning in interphase cells. J Cell Biol *162*, 963-969.

Chambers, E.L. (1939). The movement of the egg nucleus in relation to the sperm aster in the echinoderm egg. J Exp Biol *16*, 409-424.

Dent, J.A., Polson, A.G., and Klymkowsky, M.W. (1989). A whole-mount immunocytochemical analysis of the expression of the intermediate filament protein vimentin in Xenopus. Development *105*, 61-74.

Dogterom, M., Kerssemakers, J.W., Romet-Lemonne, G., and Janson, M.E. (2005). Force generation by dynamic microtubules. Curr Opin Cell Biol *17*, 67-74.

Faivre-Moskalenko, C., and Dogterom, M. (2002). Dynamics of microtubule asters in microfabricated chambers: the role of catastrophes. Proc Natl Acad Sci U S A *99*, 16788-16793.

Flemming, W. (1882). Zellsubstanz, Kern und Zellteilung.

Grill, S.W., Howard, J., Schaffer, E., Stelzer, E.H., and Hyman, A.A. (2003). The distribution of active force generators controls mitotic spindle position. Science *301*, 518-521.

Grill, S.W., and Hyman, A.A. (2005). Spindle positioning by cortical pulling forces. Dev Cell *8*, 461-465.

Hamaguchi, M.S., and Hiramoto, Y. (1986). Analysis of the role of astral rays in pronuclear migration in sand dollar eggs by the colcemid-UV method. Development Growth & Differentiation *28*, 143-156.

Herlant, M. (1911). Recherches sur les oeufs di-et-trispermiques de grenouille. *Archs Biol 26*, 103-328.

Hertwig, O. (1893). Ueber den Werth der ersten Furchungszellen fuer die Organbildung des Embryo. Experimentelle Studien am Frosch- und Tritonei. Arch mikr Anat *xlii*, pp. 662-807.

Hill, T.L., and Kirschner, M.W. (1982). Subunit treadmilling of microtubules or actin in the presence of cellular barriers: possible conversion of chemical free energy into mechanical work. Proc Natl Acad Sci USA *79*, 490-494.

J.L. Prevost, J.B.D. (1824). Nouvelle Théorie de la Génération. Annales des sciences naturelles *2*.

Kunda, P., and Baum, B. (2009). The actin cytoskeleton in spindle assembly and positioning. Trends Cell Biol *19*, 174-179.

Ledbetter, M.C., and Porter, K.R. (1963). A "Microtubule" in Plant Cell Fine Structure. J Cell Biol *19*, 239-250.

Lee, L., Tirnauer, J.S., Li, J., Schuyler, S.C., Liu, J.Y., and Pellman, D. (2000). Positioning of the mitotic spindle by a cortical-microtubule capture mechanism. Science *287*, 2260-2262.

Mitchison, T., and Kirschner, M. (1984). Dynamic instability of microtubule growth. Nature *312*, 237-242.

Morgan, T.H. (1927). Experimental embryology (Columbia Univ. Press).

Palay, S.L. (1956). Synapses in the central nervous system. J Biophys Biochem Cytol *2*, 193-202.

Pflueger, E. (1884). Ueber die Einwirkung der Schwerkraft und anderer Bedingungen auf die Richtung der Zelltheilung. Pflügers Archiv.

Rappaport, R. (1961). Experiments concerning the cleavage stimulus in sand dollar eggs. J Exp Zool *148*, 81-89.

Reinsch, S., and Karsenti, E. (1997). Movement of nuclei along microtubules in Xenopus egg extracts. Curr Biol *7*, 211-214.

Rusconi, D. (1826). Developpement de la grenouille commune depuis le moment de sa naissance jusque a son etat parfait. Giusti, Milan.

Rusconi, D. (1836). Erwiederung auf einige kritische Bemerkungen des Herrn v. Baer ueber Rusconi's Entwicklungsgeschichte des Froscheis Archiv Fuer Anatomie, Physiologie und Wissenschaftliche Medicin.

Schultze, O. (1887). Untersuchungen uber die Reifung und Befruchtung des Amphibieneies. Erste Abhandlung. Z wiss Zool *xlv*, pp. 177-226.

Slautterback, D.B. (1963). Cytoplasmic Microtubules. I. Hydra. J Cell Biol *18*, 367-388.

Swammerdam, J. (1737). Bibilia Naturae; sive historia insectorum, in classes certas redact *2*.

II. Evidence for an Upper Limit to Mitotic Spindle Length*

Martin Wühr[1#], Yao Chen[2], Sophie Dumont[1,3], Aaron C. Groen[1], Daniel J. Needleman[1], Adrian Salic[2], Timothy J. Mitchison[1]

[1]Department of Systems Biology, [2]Department of Cell Biology, Harvard Medical School, Boston, MA 02115, USA, [3]Harvard Society of Fellows, Cambridge, MA 02138

Correspondence: Martin.Wuehr@gmx.de , +1-617-230-7625

* This chapter was published in Current Biology, 2008 Aug, 26;18(16):1256-61 reprinted with friendly permission from Elsevier

Relative contributions:

MW, TJM, SD, DJN, AC designed experiments and wrote manuscript. MW performed experiments. AS, YC initiated project.

Summary

Size specification of macromolecular assemblies in the cytoplasm is poorly understood [1]. In principle, assemblies could scale with cell size, or use intrinsic mechanisms. For the mitotic spindle, scaling with cell size is expected, since the function of this assembly is to physically move sister chromatids into the center of nascent daughter cells. Eggs of *Xenopus laevis* are among the largest cells known that cleave completely during cell division. Cell length in this organism changes by two orders of magnitude (~1200 µm to ~12 µm) while it develops from a fertilized egg into a tadpole [2]. We wondered if, and how, mitotic spindle length and morphology adapt to function at these different length scales. Here, we show that spindle length increases with cell length in small cells, but in very large cells spindle length approaches an upper limit of ~60 µm. Further evidence for an upper limit to spindle length comes from an embryonic extract system that recapitulates mitotic spindle assembly in a test tube. We conclude that early mitotic spindle length in *Xenopus laevis* is uncoupled from cell length, reaching an upper bound determined by mechanisms that are intrinsic to the spindle.

Results and Discussion

Spindle length is uncoupled from cell length during first mitoses

We used immunofluorescence to measure spindle size in *Xenopus laevis* embryos fixed at different stages. Spindle length was measured at metaphase, and cell length was measured in the direction given by the pole-pole axis of the spindle (Fig. 1C). To allow comparison with meiotic spindles, which do not contain centrosomes, we defined spindle length as pole-to-pole distance, where the pole is the position where many microtubules terminate (Fig. 1C). Figure 1E shows a plot of spindle length versus cell length. At stages 8 and 9, spindle length increased with cell length but in earlier stages, and larger cells, appeared to asymptote to an upper limit of ~60 µm. Through mitoses 1 to 7, cell length decreased ~5 fold while spindle length only decreased ~1.2 fold (Fig. 1E).

Spindle morphology also changed with development, and cell length. At stages 8 and 9, centrosomes and poles were superimposed at the magnification we used, similar to the case of somatic tissue culture cells (Fig. 1A). At mitosis 7, the centrosomes appeared detached from the spindle poles at metaphase, with a relatively microtubule-sparse region connecting them (Fig. 1B). The distance between centrosomes and poles was even larger in the very early spindles (Fig. 1C) [3]. The partial disconnection of centrosomes might be a strategy of the cell to increase centrosome-to-centrosome distance when spindles reach an upper limit in length. Interestingly, the upper limit to mitotic spindle length was about

twice the length of meiotic spindles (Fig. 1D, E).

In smaller cells, where spindle length scales with cell length, we can imagine three spindle length determining mechanisms: I) Spindle length is determined extrinsically via cellular boundaries. II) A factor involved in spindle length determination is provided in limited number. Possible candidates for these factors are tubulin and MAPs that influence microtubule dynamics [4] or microtubule flux properties [5]. III) Length-regulating mechanisms that are intrinsic to the spindle systematically change during development.

The independence of spindle length from cell length we observed in very large cells suggests that spindle length is determined via a mechanism that is intrinsic to the spindle, such as microtubules dynamics or DNA content. Alternatively, spindle length may be governed by some internal boundary in the large cells that we were not able to visualize.

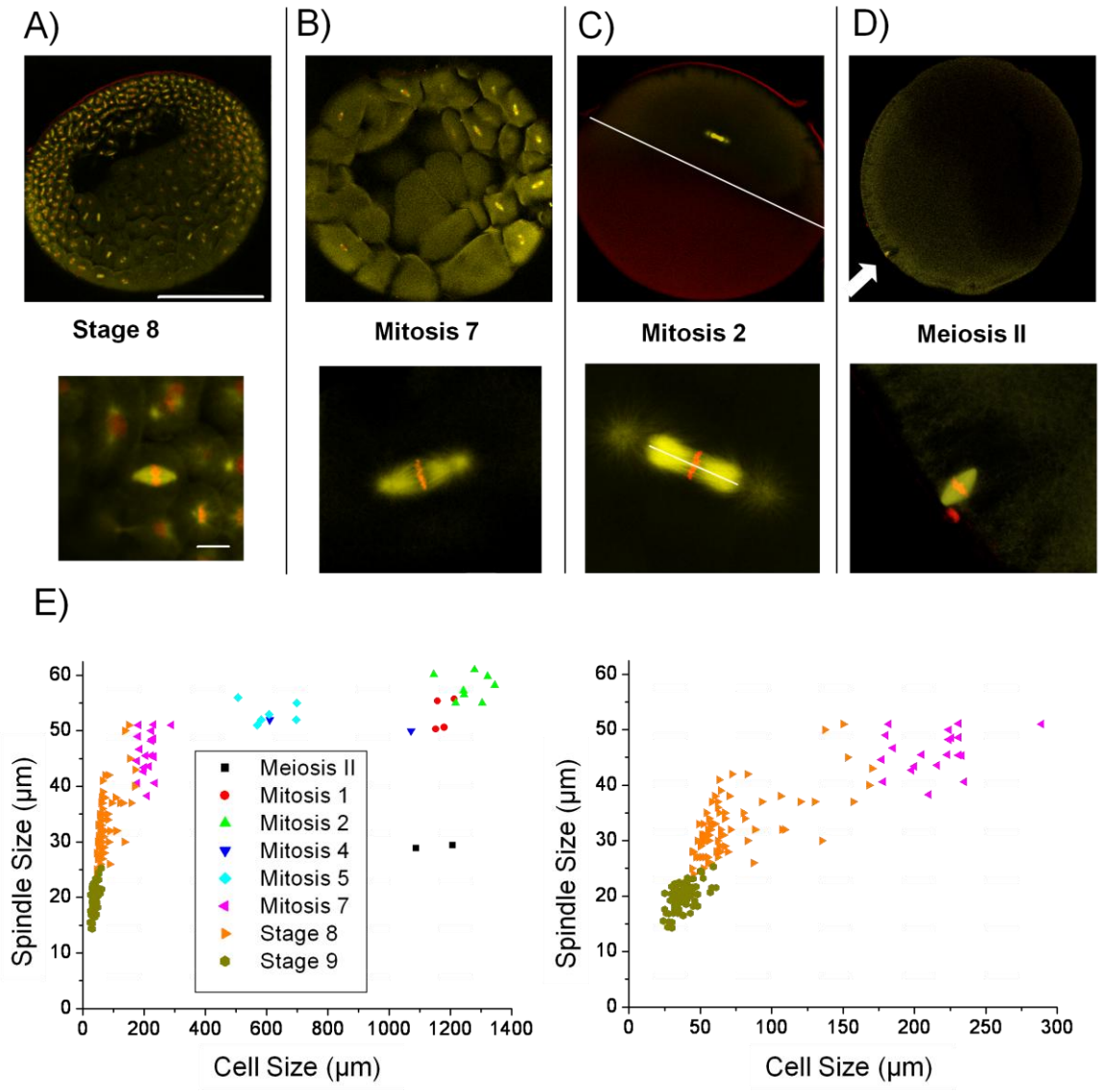

Figure II-1 Spindle size is uncoupled from cell size during first mitoses X. laevis embryos at various stages of development were fixed and stained for tubulin (yellow) and DNA (red). A) Embryo at stage 8: animal pole with smaller cells and smaller spindles on top, vegetal pole with larger cells and larger spindles on bottom. B) Embryo at mitosis 7 animal part. C) Second mitotic spindle. White lines define spindle and cell size used throughout this paper. D) Egg arrested at metaphase of meiosis II with arrow pointing at spindle. Bar for upper row = 500 µm. Bar for lower row = 20 µm. E) Plot of cell size versus spindle size at different stages of development. Spindle size increases with cell size but asymptotically reaches an upper limit ~60 µm. Plot on the right is a zoom-in of smaller cells and spindles.

Mitotic spindles in embryo extract

The standard egg extract system for spindle assembly [6] uses cytoplasm from unfertilized eggs that are arrested in meiosis II, and assembles spindles whose length and morphology closely resemble meiosis II spindles in the egg (Fig. 2A)[7]. The length of these spindle cannot be limited by the length of their container (which is a test tube), or by limiting provision of some spindle component, since mean length is insensitive to a wide range of spindle concentrations in the extract [8]. Thus, meiotic spindle length must be limited by a spindle intrinsic mechanism. To test if the same holds true for early mitotic spindles, we developed an embryo extract system that is able to recapitulate their assembly in the test tube. To avoid making a meiotic extract, it is important that the master regulator of meiosis, Mos, be degraded. We made sure that this was the case by preparing the extract from embryos that had already cleaved. By this time Mos is fully degraded [9]. Extract prepared from fertilized eggs is able to go through several cell cycles separated by ~50 minutes [10]. Though sperm nuclei condense during mitosis in this system, we observed no spindles assembling, perhaps because the extract conditions make spindle assembly slow compared to cell cycle progression. We therefore prepared extract from fertilized embryos at the two cell stage, added sperm chromatin, and incubated to allow time in interphase for chromatin assembly and DNA replication. After 80 min, we arrested the extract in mitosis by addition of the C-terminal fragment of Emi1 [11] [12]. This fragment is a potent inhibitor of the Anaphase Promoting Complex (APC), which we used rather than the standard mitotic exit inhibitor Cytostatic

Factor (CSF), since CSF extract might re-activate meiosis [13]. About 90 min after adding the APC inhibitor, spindles assembled typically with prominent astral microtubules and similar morphology to early mitotic spindles (Fig. 2B). Their length was 48 ± 6 µm (SD, n=28), comparable to mitotic spindles in early blastomeres, and significantly larger than meiotic extract spindles with a length of 32 ± 4 µm (SD) [8]. The length difference of meiotic and mitotic extract spindles appears to reflect the length differences of the *in vivo* counterparts. To our knowledge this is the first time that truly mitotic spindles could be assembled in a test tube.

Importantly, the length of these extract mitotic spindles did not scale with the test tube, strongly suggesting that early mitotic spindle length is determined by spindle intrinsic mechanisms, like meiosis II spindles, but not by a cell internal boundary. Mitotic extracts assemble spindles with comparable length to their *in vivo* counterparts, but the timing of spindle assembly was variable, and we were not able to make this system robust enough for more demanding experiments like immunodepletion or spindle assembly imaging.

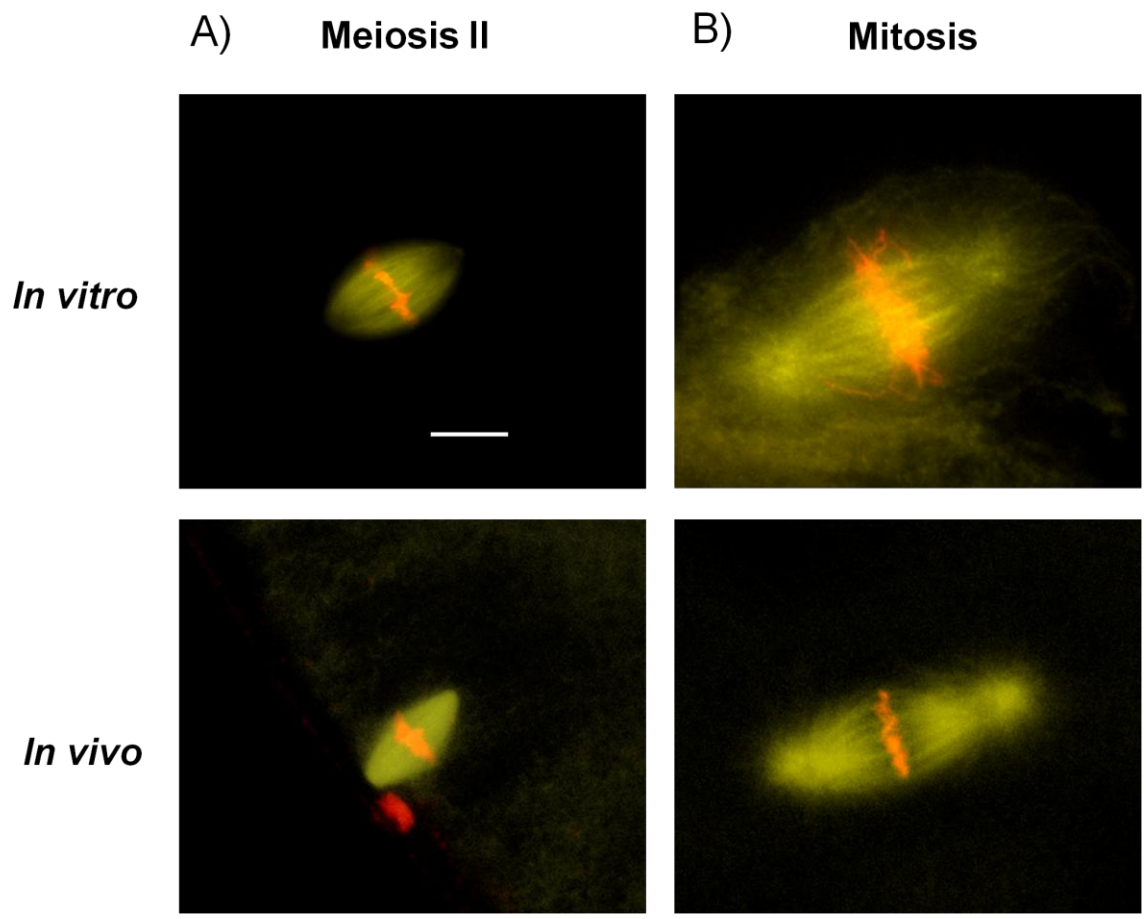

Figure II-2 Embryonic extract is able to assemble mitotic spindles DNA is shown in red and tubulin in yellow. A) Extract prepared from meiosis II arrested eggs assembles spindles that show similar morphology to meiotic in vivo spindles. B) Spindles in extract prepared from embryos were arrested in mitosis with addition of the APC-inhibitor Emil. The spindles formed show similar morphology to mitotic in vivo spindles. Bar = 20 µm.

The upper limit to spindle length is slightly sensitive to ploidy

Meiosis II spindles contain only half the number of chromosomes as larger, early mitotic counterparts, and meiotic spindle assembly depends on signals from chromatin [14]. Thus, we wondered if DNA mass plays a role in the spindle intrinsic length determination mechanism in early mitosis [15]. To test this, we

compared spindle length in haploid and diploid embryos. We found that spindles lengthen towards the onset of anaphase. To allow more accurate measurement than in Figure 1, we fixed embryos of a synchronously fertilized population between the first and second cytokineses (~112 min and ~160 min post fertilization (pf) respectively) in one minute intervals, and measured spindle length. We chose the two-cell stage because the orientation of the mitotic spindles is clearly defined by the longest cell axis (Fig. 3C), facilitating alignment of spindles in the optical plane for microscopy. By fitting the percentage of cells in anaphase to a cumulative Gaussian distribution, we calculated the most likely time for metaphase-anaphase transition at 132 ± 3 min (SD) (Fig. 3A). A linear fit of spindle length until anaphase onset revealed steady elongation of the spindle during prometaphase-metaphase at ~1.0 μm/min (Fig. 3A). We then defined the maximum metaphase length as the average measured from embryos fixed during a 5 minute window before the peak of anaphase transition. For the diploid population in Fig. 3A this value was 61.6 ± 3.1 μm (SD) (n=28). We then produced haploid embryos by fertilizing albino eggs with UV treated sperm from a pigmented male [16], and compared their spindle length to diploid embryos derived from the same parents, fertilized at nearly the same time (Fig. 3A) [17]. The large majority of UV-sperm fertilized tadpoles showed no pigment (>97 %), and a phenotype typical of haploids (Fig. 4A) [18, 19]. Haploidy was further confirmed by counting chromosomes (data not shown). At the two-cell stage, the UV-treated sperm nucleus, with few microtubule associated, was typically observed away from the spindle (Arrow Fig. 3C). Only one free nucleus was

observed, indicating that UV treatment inhibited replication.

Average spindle length was measured as 55.2 ± 3.9 µm (SD, n=14) for haploids and 62.1 ± 3.1 µm (SD, n=12) for diploids (Fig. 3D). A t-test resulted in a p-value of 0.005 % making the small difference statistically significant. We conclude that the upper limit to mitotic spindle size can be reduced by ~10 % by halving the amount of DNA. This difference is similar to the DNA-dependent length difference observed in meiotic extract spindles [20]. Thus, signaling from chromatin may contribute to spindle length control in meiotic and mitotic spindles, but it does not appear to be a major factor governing length. Haploid mitotic spindles were about two-fold longer than meiosis II spindles (Fig. 1C, D, E) that contain the same amount of DNA, showing that ploidy alone cannot account for length differences between meiosis and mitosis.

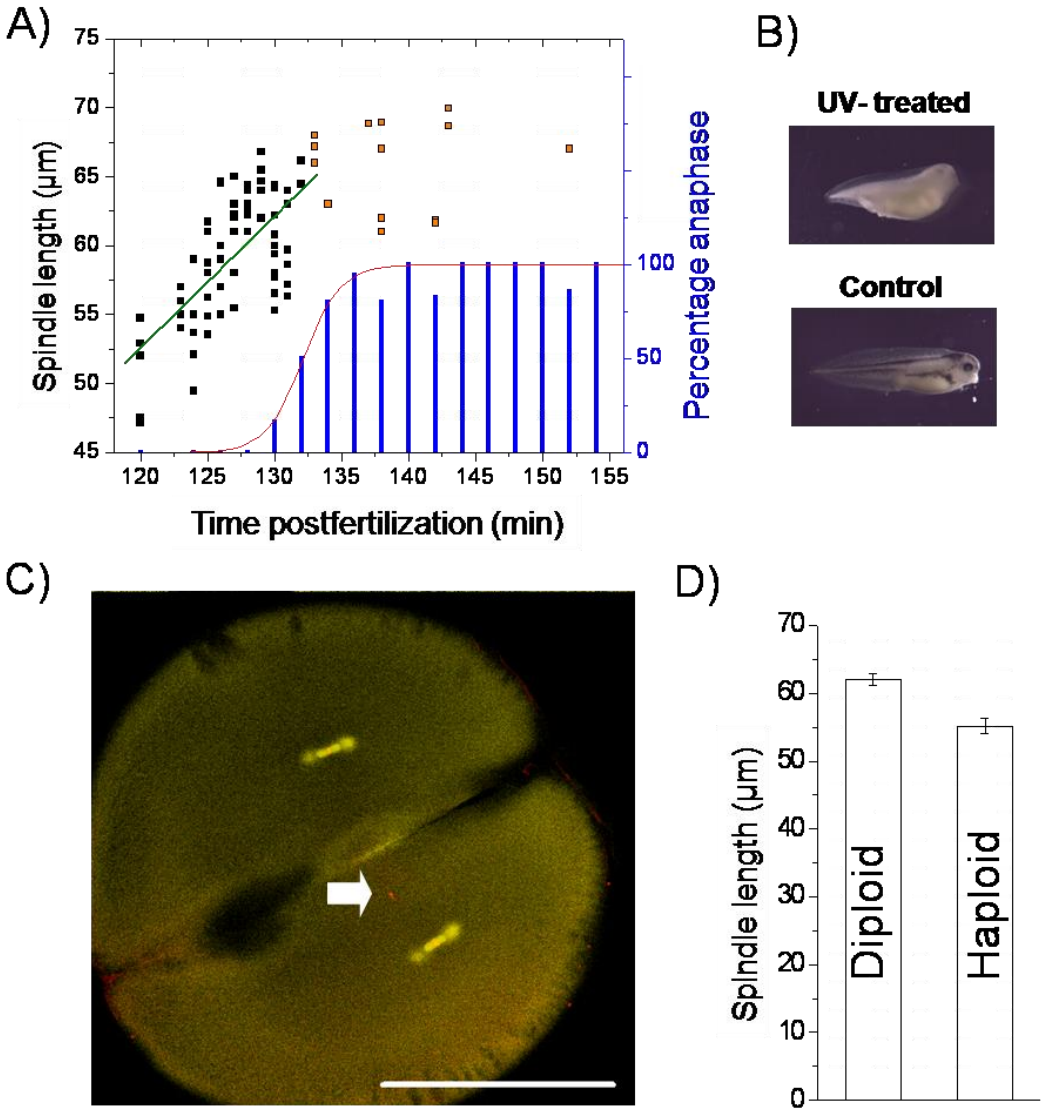

Figure II-3 Halving the DNA content reduces spindle length by ~10%.

A) Percentage of embryos (synchronously fertilized) in anaphase (blue bars) was fitted to a cumulative Gaussian distribution (red line), calculating the time for metaphase-anaphase transition at 132 ± 3 min (SD). Spindle length before peak of anaphase onset (black squares) was fitted linearly (green line) revealing spindle growth of 1.0 µm/min. Delayed spindles (shown as orange squares) were ignored for growth measurement as this would have systematically underestimated growth rate. B) Albino eggs were fertilized with UV-treated sperm from a pigmented male resulting in tadpoles with no pigments but haploid phenotype. Control developed with pigments and diploid phenotype C) Sperm derived DNA (arrow) is separate from spindles at two-cell stage of haploid embryo. Bar = 500 µm. D) Spindle mean length for haploids is 55.2 µm and therefore ~10 % shorter than diploids with 62.1 µm. Standard errors are 0.9 µm and 1.1 µm, respectively, with a statistically significant p-value of 0.005 %.

Relatively small spindles undergo long, fast anaphase B-like movement

How can a spindle that is only 1/20th of the cell length (Fig. 1E) segregate chromosomes to the center of the daughter cells? To find out, we fixed synchronously fertilized populations at different time intervals at the two cell stage, and observed the distribution of DNA and microtubules. At the onset of anaphase, astral microtubules started to extend (Fig. 4A,B), rapidly forming a hollow structure, where (presumed) plus ends move out towards the cortex, but many minus ends apparently move out at roughly the same rate. Chromosomes stayed condensed, and were surrounded by bright stain for tubulin, until they had separated by ~180 µm (Fig. 4B). At approximately this distance the nuclear envelope reformed, but the DNA continued to separate to a final distance of ~400µm. By this time, astral microtubule plus ends were touching the cell cortex, and the second cytokinesis is initiated (Fig. 4C). Sister DNA separation during anaphase was plotted versus time (Fig. 2D). A linear fit showed a distance increase of ~15 µm/minute (Fig. 2D), with no obvious difference in separation rate for condensed or uncondensed DNA. This is fast compared to ~4 µm/min observed for anaphase-B movement in HeLa cells [21].

To test whether actin is involved in the separation of the DNA [22], we observed fixed embryos that had been incubated with the F-actin capping drug Cytochalasin B (33 µg/ml) [23]. This resulted in inhibition of cytokinesis, but spindle assembly and separation of DNA were not measurably perturbed (Fig. 4E). However, while the drug did block cleavage, it is possible that its

concentration was insufficient to block actin dependent processes deep in the embryo, so our conclusion that F actin is not required for DNA separation is provisional.

Our measurements in large cells, and extract experiments, suggest that Xenopus early mitotic spindle length is determined via an intrinsic mechanism that sets an upper length of ~60 µm. This limit was reduced by ~10 % in haploid spindles, suggesting signals from DNA contribute to setting length, but are not a major factor. Recently, we proposed a model for meiotic spindle length regulation in which length depends primarily on a balance between microtubule nucleation-loss and transport by motors [5]. Perhaps a spindle intrinsic mechanism of this kind also operates in mitotic spindles.

Relatively small spindle size in large cells requires adaptation of the mitotic process, which includes an unusually long and fast anaphase B, and perhaps also partial separation of centrosomes from the spindle. One question puzzles us greatly: how can the relatively small spindle orient itself in the large cell to specify the next cleavage plane perpendicular to the longest cell axis (Fig. 3C) [24],[25],[26]? In more ordinary sized cells, spindle orientation is thought to require contact of astral microtubules with the cortex [27],[28]. Perhaps some microtubules are long enough to reach cortex during prometaphase-metaphase of early Xenopus mitosis, but this seems unlikely because these microtubules would have to be much longer than the spindle microtubules, and they would

have to elongate to the cortex much faster than the astral microtubules that grow out at anaphase (~15 μm/min, estimated from images like those in Figure 4). Rather, we suspect some uncharacterized spindle orientation mechanism must exist. Perhaps the astral microtubules at late anaphase can sense the longest cell axis and determine centrosome orientation for the next spindle.

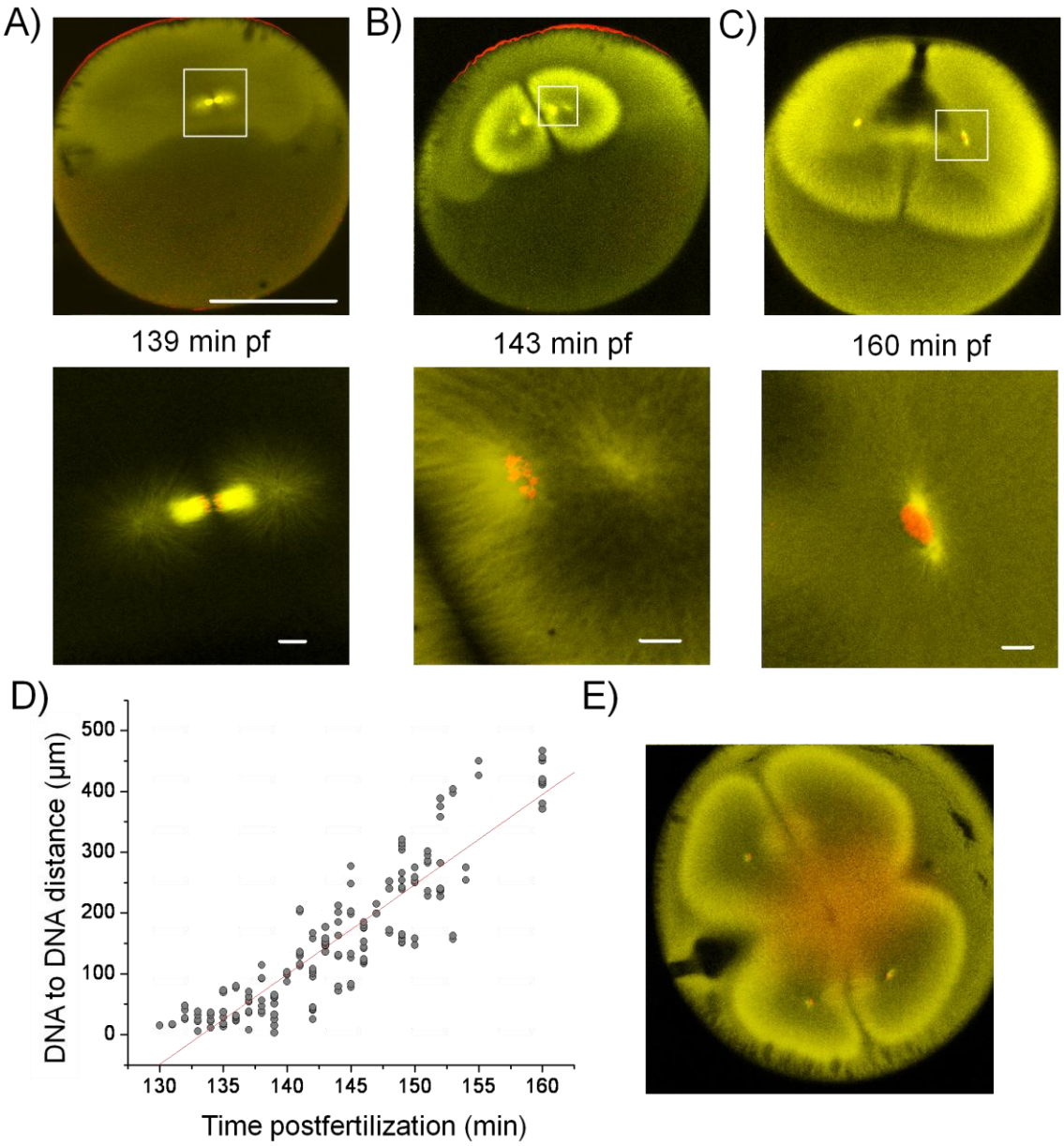

Figure II-4: Relatively small spindle is compensated by enormous anaphase B like movement

Embryos of a synchronously fertilized population were fixed between first and second cytokineses and stained for tubulin (yellow) and DNA (red). A) At anaphase the astral microtubules start to elongate. B) Up to a DNA to DNA distance of ~180 µm, DNA is still condensed and surrounded by high staining of microtubules. Astral microtubules form a hollow structure. C) Nuclear envelope has reformed and finally the nuclei have been separated by ~400 µm, astral microtubules reach the cell cortex and cytokinesis starts. A-C) Bar for upper row = 500 µm, Bars in lower row = 20 µm. D) Plot of DNA to DNA distance versus time. Linear fit estimates speed of DNA separation at ~15 µm/min. E) Cytokinesis, but not separation of DNA, is inhibited by addition of 33 µg/ml of actin depolymerazing Cytochalasin B.

Experimental Procedures

Immunofluorescence of embryos

Embryos were raised at 16º C. Previous protocols [29] were modified as follows. Embryos were fixed in 50 mM EGTA, 10 % H_2O, 90 % methanol for at least 12 h. Pigmented embryos were bleached in 10 % H_2O_2, 20 % H_20, and 70 % methanol under illumination for 24 hours. Specimen were dehydrated with a series of 20 %, 40 %, 80 % 100 % TBS/Methanol. For hemisection embryos were cut in TBS on an agarose cushion with a scalpel. Specimen were incubated with directly labeled α-tubulin antibody (T6074 (sigma) 4.6/AB labeling ratio, Alexa 547 (Invitrogen)) 1:100 for at least 12 h at 4º C in TBSN (TBS + 0.1 % Nonidet P40 + 0.1 % sodium azide, 2 % BSA, 1 % FCS). Embryos were washed in TBSN for at least 24 hours. DNA was stained with YoPro3 (Invitrogen) (5mM) or To-Pro-1 (Invitrogen) (5mM) in TBSN for 30 min and washed in TBSN for 1h. After one wash in TBS and two changes of methanol embryos were cleared in Murray's clear (benzyl benzoate, part benzyl alcohol 2:1)and mounted in metal slides with a hole (thickness of 1.2 mm for whole mount or 0.8 mm for hemisected). The hole was closed on the bottom with parafilm attached coverslip. Microscopy was performed on an upright Biorad Radiance 2000 or inverted Zeiss Meta 550 with 10 x (0.3 NA) or 20 x (0.75 NA) objectives.

Comparison of haploid and diploid spindle length

To generate haploid embryos half a testis was macerated with an Eppendorf pestle in 1ml of MMR and pressed with a syringe through cheese cloth to remove tissue junks. The suspension was placed on a Petri dish with 7 cm diameter and irradiated 2 times at 30,000 microjoules/cm^2 with swirling in between in a UV Stratalinker 2400 [30]. Embryos were fertilized with this suspension and fixed at the two cell stage, hemisected along the first cleavage plane and prepared for immunofluorescence as described above. Spindle size within one embryo is more similar than spindles in the whole population. Therefore for the t-test (ttest2 function in Matlab (Mathworks)) the average spindle length per embryo was used. Karyotyping was performed as described [31]. Curve fitting was performed with cftool in Matlab (Mathworks).

Embryo extract spindles

Published protocols [32],[6] for meiotic extract spindles were modified as follows to give mitotic extract spindles. Females were squeezed, eggs fertilized and dejellied. Embryos from different animals were kept separate and only if fertilization rate was close to 100% embryos were used. After the first cleavage non-fertilized eggs were sorted out because of dominant effect of CSF. Embryos were washed in XB (100 mM KCl, 0.1mM CaCl2, 1mM $MgCl_2$, 10 mM Hepes, 50 mM Sucrose, pH 7.8 (KOH)). 0.75 ml of silicon oil AP100 (Fluka) were added to a 50Ultra-Clear Tube (11x34mm) (Beckmann), embryos were transferred to top, incubated for 15 min on ice, and spun at 2000 rpm in a JS4.2 (Beckmann) for 4

min at 4º C. Buffer and oil were removed. Embryos were crushed at 12000rpm in a TLS-55 (Beckmann) for 15 min at 4 º C. The cyotplasmic fraction was removed with a syringe. A clearing spin in a tabletop centrifuge at 4º C, 4 min, 12000g followed to remove residual oil. Cytochalasin D (10µg/ml), LPC (10 µg/ml each of leupeptin, pepstatin, chymostatin) and Energy Mix (7.5 mM creatine phosphate,1 mM ATP, 0.1 mM EGTA, 1 mM MgCl2) were added. Demembrenated sperm was added and extract allowed to cycle at RT. After ~80 min bacterially expressed C-terminal fragment of EmiI (23mg/ml) was added at 1:200. Spindles typically formed after an additional 90 minutes. C-terminal fragment of EmiI was purified via a His-tag and frozen in XB + 200 mM KCl.

Acknowledgements

We would like to thank Jagesh Shah, Andrew Murray, Marc Kirschner, Rebecca Ward, Yifat Merbl, Tom Maresca, Jay Gatlin, Cell division group Woods Hole, Eva Kiermaier and people in the Mitchison lab for helpful suggestions and discussion, Olaf Stemmann for training, Michael Rape for plasmid of EmiI, Jim Horn for technical assistance, Nikon Imaging Center (HMS) and Zeiss Woods Hole for imaging assistance. DJN was supported by the Life Sciences Research Foundation, sponsored by Novartis.This work was supported by the National Institutes of Health (NIH) grants GM39565 and P50 GM068763-1.

References

1. Marshall, W.F. (2004). Cellular length control systems. Annu Rev Cell Dev Biol *20*, 677-693.

2. Montorzi, M., Burgos, M.H., and Falchuk, K.H. (2000). Xenopus laevis embryo development: arrest of epidermal cell differentiation by the chelating agent 1,10-phenanthroline. Mol Reprod Dev *55*, 75-82.

3. Gard, D.L., Cha, B.J., and Schroeder, M.M. (1995). Confocal immunofluorescence microscopy of microtubules, microtubule-associated proteins, and microtubule-organizing centers during amphibian oogenesis and early development. Curr Top Dev Biol *31*, 383-431.

4. Andersen, S.S., Ashford, A.J., Tournebize, R., Gavet, O., Sobel, A., Hyman, A.A., and Karsenti, E. (1997). Mitotic chromatin regulates phosphorylation of Stathmin/Op18. Nature *389*, 640-643.

5. Burbank, K.S., Mitchison, T.J., and Fisher, D.S. (2007). Slide-and-cluster models for spindle assembly. Curr Biol *17*, 1373-1383.

6. Sawin, K.E., and Mitchison, T.J. (1991). Mitotic spindle assembly by two different pathways in vitro. J Cell Biol *112*, 925-940.

7. Lohka, M.J., and Maller, J.L. (1985). Induction of nuclear envelope breakdown, chromosome condensation, and spindle formation in cell-free extracts. J Cell Biol *101*, 518-523.

8. Mitchison, T.J., Maddox, P., Gaetz, J., Groen, A., Shirasu, M., Desai, A., Salmon, E.D., and Kapoor, T.M. (2005). Roles of polymerization dynamics, opposed motors, and a tensile element in governing the length of Xenopus extract meiotic spindles. Mol Biol Cell *16*, 3064-3076.

9. Sagata, N., Watanabe, N., Vande Woude, G.F., and Ikawa, Y. (1989). The c-mos proto-oncogene product is a cytostatic factor responsible for meiotic arrest in vertebrate eggs. Nature *342*, 512-518.

10. Murray, A.W., and Kirschner, M.W. (1989). Cyclin synthesis drives the early embryonic cell cycle. Nature *339*, 275-280.

11. Reimann, J.D., Freed, E., Hsu, J.Y., Kramer, E.R., Peters, J.M., and Jackson, P.K. (2001). Emi1 is a mitotic regulator that interacts with Cdc20 and inhibits the anaphase promoting complex. Cell *105*, 645-655.

12. Schmidt, A., Rauh, N.R., Nigg, E.A., and Mayer, T.U. (2006). Cytostatic factor: an activity that puts the cell cycle on hold. J Cell Sci *119*, 1213-1218.

13. Moses, R.M., and Masui, Y. (1989). Cytostatic Factor (Csf) in the Eggs of Xenopus-Laevis. Experimental Cell Research *185*, 271-276.

14. Heald, R., Tournebize, R., Blank, T., Sandaltzopoulos, R., Becker, P., Hyman, A., and Karsenti, E. (1996). Self-organization of microtubules into bipolar spindles around artificial chromosomes in Xenopus egg extracts. Nature *382*, 420-425.

15. Nicklas, R.B., and Gordon, G.W. (1985). The total length of spindle microtubules depends on the number of chromosomes present. J Cell Biol *100*, 1-7.

16. Reinschmidt, D.C., Simon, S.J., Volpe, E.P., and Tompkins, R. (1979). Production of Tetraploid and Homozygous Diploid Amphibians by Suppression of 1st Cleavage. Journal of Experimental Zoology *210*, 137-143.

17. Noramly, S., Zimmerman, L., Cox, A., Aloise, R., Fisher, M., and Grainger, R.M. (2005). A gynogenetic screen to isolate naturally occurring recessive mutations in Xenopus tropicalis. Mech Dev *122*, 273-287.

18. Hamilton, L. (1963). An Experimental Analysis of Development of Haploid Syndrome in Embryos of Xenopus Laevis. Journal of Embryology and Experimental Morphology *11*, 267-&.

19. Porter, K.R. (1939). Androgenetic development of the egg of Rana pipiens. Biological Bulletin *77*, 233-257.

20. Brown, K.S., Blower, M.D., Maresca, T.J., Grammer, T.C., Harland, R.M., and Heald, R. (2007). Xenopus tropicalis egg extracts provide insight into scaling of the mitotic spindle. J Cell Biol *176*, 765-770.

21. Mayr, M.I., Hummer, S., Bormann, J., Gruner, T., Adio, S., Woehlke, G., and Mayer, T.U. (2007). The human kinesin Kif18A is a motile microtubule depolymerase essential for chromosome congression. Curr Biol *17*, 488-498.

22. Verlhac, M.H., Lefebvre, C., Guillaud, P., Rassinier, P., and Maro, B. (2000). Asymmetric division in mouse oocytes: with or without Mos. Curr Biol *10*, 1303-1306.

23. Gard, D.L., Cha, B.J., and Roeder, A.D. (1995). F-actin is required for spindle anchoring and rotation in Xenopus oocytes: a re-examination of the effects of cytochalasin B on oocyte maturation. Zygote *3*, 17-26.

24. Hertwig, O. (1893). Ueber den Werth der ersten Furchungszellen f ur die Organbildung des Embryo. Experimentelle Studien am Frosch- und Tritonei. Arch. mikr. Anat. *xlii*, pp. 662-807.

25. Born, G. (1893). Ueber Druckversuche an Froscheiern. Anat. Anz. *viii*, pp. 609-627.

26. Sawai, T., and Yomota, A. (1990). Cleavage plane determination in amphibian eggs. Ann N Y Acad Sci *582*, 40-49.

27. Strauss, B., Adams, R.J., and Papalopulu, N. (2006). A default mechanism of spindle orientation based on cell shape is sufficient to generate cell fate diversity in polarised Xenopus blastomeres. Development *133*, 3883-3893.

28. Thery, M., Jimenez-Dalmaroni, A., Racine, V., Bornens, M., and Julicher, F. (2007). Experimental and theoretical study of mitotic spindle orientation. Nature *447*, 493-496.

29. Becker, B.E., and Gard, D.L. (2006). Visualization of the cytoskeleton in Xenopus oocytes and eggs by confocal immunofluorescence microscopy. Methods Mol Biol *322*, 69-86.

30. Tompkins, R. (1978). Triploid and Gynogenetic Diploid Xenopus-Laevis. Journal of Experimental Zoology *203*, 251-256.

31. Hirsch, N., Zimmerman, L.B., Gray, J., Chae, J., Curran, K.L., Fisher, M., Ogino, H., and Grainger, R.M. (2002). Xenopus tropicalis transgenic lines and their use in the study of embryonic induction. Dev Dyn *225*, 522-535.

32. Desai, A., Murray, A., Mitchison, T.J., and Walczak, C.E. (1999). The use of Xenopus egg extracts to study mitotic spindle assembly and function in vitro. Methods Cell Biol *61*, 385-412.

III. How does a millimeter-sized cell find its center?*

Martin Wühr[#1], Sophie Dumont[1,3], Aaron C. Groen[1], Daniel J. Needleman[2], Timothy J. Mitchison[1]

[1]Department of Systems Biology, Harvard Medical School, Boston, MA 02115,

[2]FAS Center for Systems Biology, Harvard University, Cambridge, MA 02138

[3]Harvard Society of Fellows, Cambridge, MA 02138

* This chapter was published in Cell Cycle 2009 Apr 15;8(8):1115-21, reprinted with friendly permission from Landes Bioscience.

Relative contribution:

MW performed experiments. MW, TJM, SD, DJN and AG wrote manuscript.

Abstract

Microtubules play a central role in centering the nucleus or mitotic in eukaryotic cells. However, despite common use of microtubules for centring, physical mechanisms can vary greatly, and depend on cell size and cell type. In the small fission yeast cells, the nucleus can be centered by pushing forces that are generated when growing microtubules hit the cell boundary. This mechanism may not be possible in larger cells, because the compressive force that microtubules can sustain are limited by buckling, so maximal force decreases with microtubule length. In a well-studied intermediate sized cell, the *C. elegans* fertilized egg, centrosomes are centered by cortex-attached motors that pull on microtubules. This mechanism is widely assumed to be general for larger cells. However, re-evaluation of classic experiments in a very large cell, the fertilized amphibian egg, argues against such generality. In these large eggs, movement of asters away from a part of the cell boundary that they are touching cannot be mediated by cortical pulling, because the astral microtubules are too short to reach the opposite cell boundary. A century ago, Herlant and Brachet discovered that multiple asters within a single egg center relative to the cell boundary, but also relative to each other. Here, we summarize current understanding of microtubule organization during the first cell cycle in a fertilized *Xenopus* egg, discuss how

microtubule asters move towards the center of this very large cell, and how multiple asters shape and position themselves relative to each other.

Introduction:

Eukaryotic cells come in many shapes and sizes, but a common feature is that the interphase nucleus, and the mitotic spindle, are positioned in a specific location. This is usually the center of the cell, but off-center locations are common in specific biological circumstances, such as asymmetric division during embryogenesis. The mechanism for this centering is a fundamental question of cellular organization that has long puzzled cell biologists. Microtubules appear to play a key role, perhaps because they are one of the few cellular structures whose length scale approaches that of the whole cell, and also because their rapid polymerization dynamics allow them to explore the entire cytoplasmic space[1]. Microtubule-based force-generating mechanisms, that use polymerization dynamics and motor proteins, are conserved in all eukaryotes, yet microtubule-based centering mechanisms may not be. One reason for this is strong physical constraints on the length scales over which potential force-generating mechanisms can operate. Because of these constraints, fundamentally different centering mechanisms may operate in cells of different sizes. Recent research has addressed centering mechanisms mainly in rather small cells, exemplified by fissions yeast (length ~10μm) and medium-sized cells,

exemplified by the *C. elegans* fertilized egg (length ~45 µm). Here, we discuss a much larger cell, the fertilized amphibian egg, whose much larger size (length ~1200 µm in *Xenopus*), we argue, demands novel mechanisms. These large-cell mechanisms are interesting in their own right, and they also illuminate aspects of cytoplasmic organization that may be generally relevant.

In the small fission yeast cell, the nucleus is centered by pushing forces that are generated when microtubules growing outwards from the nucleus encounter the cell boundary[2]. It is thought that this mechanism cannot work to center nuclei or spindles in larger cells because the maximal compressive force that microtubules can sustain drops in proportion to the square of their length. This 1/length^2 argument holds for an elastic rod in liquid; the situation may be more complex in cytoplasm because embedding an elastic rod in an elastic gel increases the compressive force it can sustain[3], and microtubule bundles can also sustain larger forces. Despite these potential caveats, both fundamental constraints from buckling, and direct experimental observation, support the view that centration of asters and nuclei in *C. elegans* eggs is driven by pulling forces on microtubules generated by minus end directed motors (presumably dynein) attached to the cell cortex [4-6]. Pulling by cortical dynein also moves nuclei in small budding yeast cells[7], though the strong asymmetry of those cells, associated with the budding cycle, make them not directly applicable to a discussion of centering. Dynein activity is also required for mitotic spindle and nucleus centering in mammalian

tissue culture cells [8, 9]. Because of that kind of data, and the elegance of the *C. elegans* work, pulling by minus end directed motors at the cortex seems to be accepted as the general mechanism of centering in larger cells[10, 11]. By reviewing older work, confirmed with new micrographs, we show that the cortical pulling model for aster centering cannot hold in a very large cell, the fertilized amphibian egg. We discuss alternative models, and their broader implications for cytoplasmic organization.

Microtubule organization during the first cell cycle in fertilized Xenopus eggs

To set the stage for a discussion of centering mechanisms, we will first review microtubule organization during the first cell cycle in fertilized eggs of the clawed frog *Xenopus laevis*. Egg diameter in this species is ~ 1200 µm, which is ~ two orders of magnitude larger in length than typical cells in animal tissues[12]. Some amphibian have even larger eggs[13]. Time is normalized to fertilization (defined as 0) and first cleavage (defined as 1)[14]. Typical absolute values for the 0-1 interval is ~90 min at 23^0C. The lower portion of a *Xenopus* egg is packed with large yolk granules, creating a density asymmetry that makes the egg orient under gravity[15]. The lowest part of the egg is called the vegetal pole, and the upper part the animal pole. In *Xenopus*, the animal half of the egg is brown-black due dark pigment in the cortex, while the vegetal half is white. Because of the packed yolk

in the vegetal half of the egg, the distribution of free cytoplasm is not spherical, but looks more like a flattened hemisphere (Fig. 1). In discussing models for centering, we will neglect the vertical dimension, and concentrate on a horizontal plane through this hemisphere of cytoplasm, as shown in figure 1. All the following picture and cartoons depict positioning and movement in this plane. Asters can also move somewhat in the vertical plane, and we assume they do so by mechanisms similar to movement in the horizontal plane.

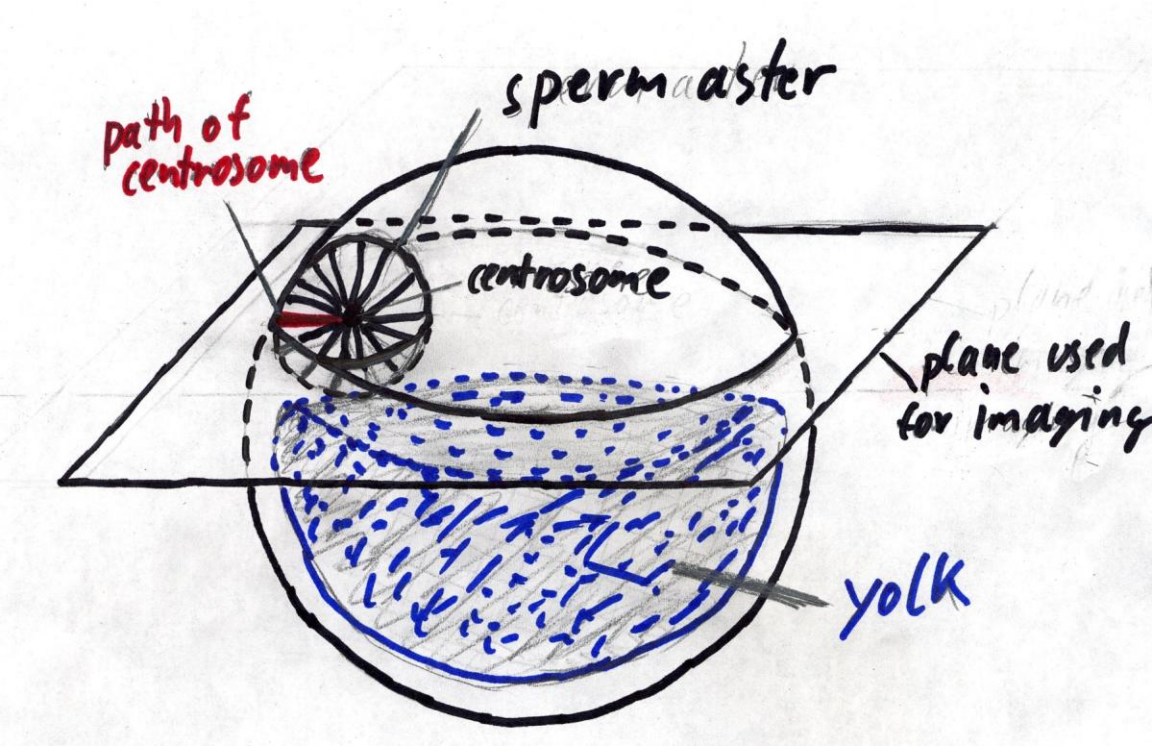

Figure III-1: Cartoon of a frog egg shortly after fertilization. The vegetal part (bottom) is heavily filled with yolk. The sperm enters randomly at the animal (top) part of the egg. The radial grow of the sperm aster leads to the movement of the centrosome towards the cell's center. All micrograph in this paper were taken in the plane shown.

Before fertilization, the egg is arrested in metaphase of meiosis II with a relatively small meiotic spindle attached to the cortex at the animal pole of the egg[16]. Sophisticated mechanisms ensure that only one sperm enters the egg, in the animal hemisphere[17]. Fertilization generates a wave of elevated Ca++ in the cytoplasm that triggers anaphase in the meiotic spindle followed by extrusion of half the maternal DNA into the second polar body. The sperm carries the male DNA and two centrioles, which form a microtubule organizing center that initiates outgrowth of a dense radial array of microtubules with their plus ends presumably oriented outwards[18]. This structure is called the sperm aster (Fig. 1 and 2 A). The sperm aster's diameter increases at a rate we estimate from images of embryos fixed at different times as ~30 µm/min. By ~0.5 the sperm aster grows to the point that its plus ends come close to the cortex all around the circle defined by the plane in figure 1[5]. By this time, the centrosomes have moved towards the center of the cell (Fig. 2B)[19, 20]. The centering is not perfect; they tend to be closer to the site of sperm entry than the opposite side (Fig 2 B and C), but it is clear they have moved a long way from where the sperm entered the egg, at least 300 µm in most cases. Below, we will discuss models for how this centering movement of the centrosomes might be driven.

As soon a microtubules from the sperm aster reach the female nucleus, it starts to move towards the center of the aster, presumably pulled by dynein attached to

the nuclear envelope[21]. In this way, the male and female pronuclei meet close to the centrosomes.

As the first mitosis is initiated, both nuclear envelopes, and the sperm aster, disassemble, and a mitotic spindle assembles (Fig. 2 C)[22]. In smaller cells, such as the *C. elegans* egg, the mitotic spindle finds the center of the cell using long astral microtubules[9], but in the frog egg is clear that the sperm aster is responsible for moving both the centrosomes and the DNA to approximately the cell's center, and the spindle then forms in that spot. The metaphase spindle probably could not center itself in the frog egg, because its astral microtubules are much shorter than the radius of the egg (Figure 2C)[22, 23].

At anaphase, the sister chromatids separate, and the astral microtubules of the spindle start to grow out rapidly; again we estimate an elongation rate of ~15μm/min based on fixed images. Anaphase chromosome movement presumably starts with a conventional, kinetochore-based anaphase-A. Anaphase-B movement in these large egg cells is atypical, presumably to allow a large segregation distance when spindles are small relative to the egg. The sister DNA masses move apart rapidly over a distance much larger than the metaphase spindle length, the reach a position ~half way between the center of the egg and its periphery (figure 2D). This requires that the DNA masses move ~250 μm in ~25 min. Approximately half this movement occurs while the DNA is still condensed, and half after the nuclear envelope has reformed[23]. The origin of

the forces that drive and direct this large anaphase-telophase segregation movement are unclear. The centrosomes are positioned a few tens of microns ahead of the moving nuclei, and appear to be pulling them, but it is far from clear why the centrosomes move apart in a straight line that is parallel to the spindle axis. Because these movements can be viewed as asters moving towards the center of a volume of cytoplasm, we suspect they may be driven by the same forces that cause centering of the sperm aster, which we discuss below.

The paired asters, we here call telophase-asters, originate in the centrosomes of the anaphase mitotic spindle and not only move the sister nuclei apart but are also responsible for determining the cleavage plane. It is believed that the site of cleavage furrow ingression is specified by a line along the cortex, normal to the direction of chromosome segregation, where the two antiparallel arrays of microtubules from the pair of asters come together the cortex [24].

Besides their role in cell division and chromosome separation, microtubules are also involved in determining the future dorso-ventral axis of the embryo. In this paper we would like to concentrate on microtubules involved in centering. Detailed descriptions of microtubules involved in setting up dorso-ventral axes are presented elsewhere[25-27].

An interesting aspect of the organization of both the sperm aster (Fig. 2 A and B), and the subsequent telophase asters (Fig. 2 D) is that they appear hollow in tubulin immunofluorescence images[28], as if many of the microtubules in the periphery of the aster do not have their minus ends located near the centrosome. We do not think this hollow aster image is an artifact of fixation or stain penetration, because higher microtubules density close to the outline of the asters can not only be seen near the egg's surface but also deep inside (Fig. 2 D and 4 B). Also, we think it physically impossible that all the microtubules with plus ends at the periphery of the aster could have minus ends close to the centrosome, because of physical packing constraints. If all microtubules were continuous from center to periphery, their density in a plane tangential to the aster would have to scale as $1/\text{radius}^2$ as the plane moved outwards from the center, and as 1/radius in a plane that cut through the center of the aster. Our immunofluorescence images are completely inconsistent with this relationship, since the asters get brighter towards the outside not dimmer. We presume a subset of the astral microtubules are nucleated at centrosomes and run continuously out to the periphery, since the centrosome stays in the center of the aster as the aster moves and expands, implying the centrosome is physically connected to the aster periphery. But we believe that the majority of microtubules in these asters must have a different origin. Perhaps they are nucleated from the sides of existing microtubules, pointing in the same direction, for example. Microtubules are nucleated in the absence of centrosomes in egg meiotic spindles, and in this case too it may be important that new microtubules point in

the same direction as the majority of microtubules near them, to preserve the gradient of polarity in each half spindle[29]. We suspect that both situations require a biochemical mechanism that nucleates new microtubules in the vicinity of old ones, and pointing in the same direction.

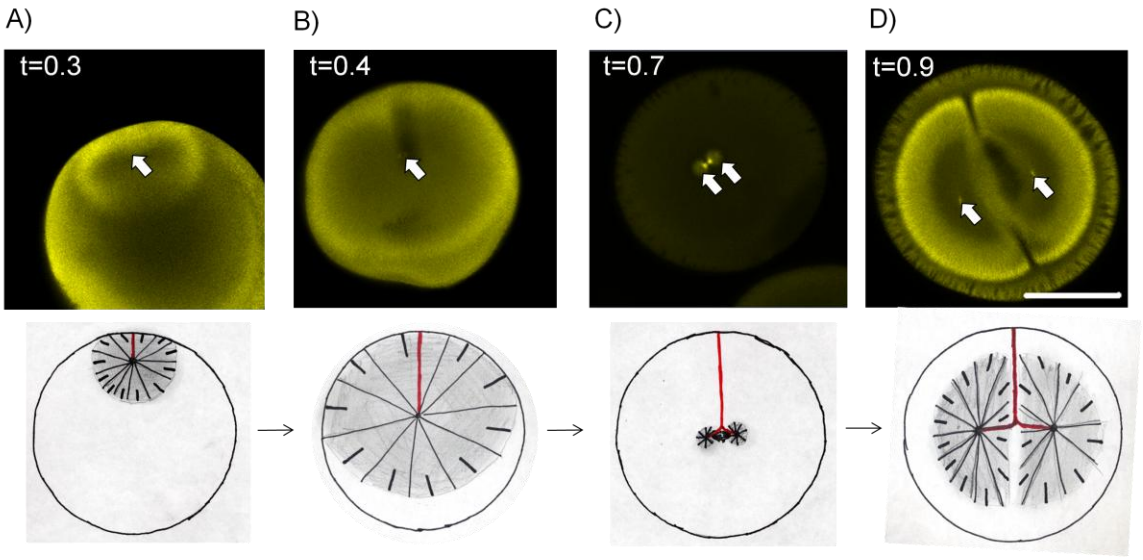

Figure III-2: Overview of microtubule organization during the first cell cycle in *X. laevis*. Top: Immunostaining against tubulin, bar = 500 µm. Arrows indicate positions of centrosomes. Time (t) is normalized to first cleavage. Bottom: cartoon of corresponding time with the path of the centrosome in red and microtubules in black. A) and B) Growth of sperm aster moves centrosome towards the center of the cell. C) After sperm aster breaks down first mitotic spindle forms D) At telophase the astral microtubules grow out and the centrosomes are moved to the centers of the future daughter cells.

How might asters center?

As discussed above, both the sperm aster and the telophase asters move towards the center of a volume of cytoplasm that is not occupied by microtubules. In the case of the sperm aster, it alone occupies that volume, and it

moves to the center, while in telophase two asters move apart from each other, to a position half way between the periphery and the other aster. We will now evaluate four potential models to account for the forces that drive and direct these centralizing movements: A) Simple microtubule pushing B) Pushing with a stiffened microtubule meshwork C) Pulling from the cortex with limited attachment sites. D) Pulling on the cytoplasm.

A) *Simple microtubule pushing*. In this model, individual astral microtubules nucleated from the centrosome push against the cortex or yolk granules in the cytoplasm [30]. The pushing force is generated by plus end polymerization against a barrier, which is believed to be the main mechanism for centering the interphase nucleus in the fission yeast *S. pombe*[2]. The compressive force a microtubule can sustain before it buckles, called the Euler force ($F_{e)}$ is given by[30]:

1) $$F_e = \frac{C \times R^4}{L^2}$$

Where *R* is the radius of the rod, *L* is its length and *C* is a material-dependent constant. Centering can be achieved by one of two mechanisms: either the microtubule only push off against one side because that side is closer, or they push off against both sides, but the force is less on the long side because

microtubules have a greater tendency to buckle on the long side (Fig. 3A). The estimated force required to move an intermediate sized aster with 200 μm radius through the cytoplasm at observed rates was ~100 pN[31]. For comparison, the maximal force that can be transmitted by a single microtubule 200 μm long is ~8 fN[31]. One therefore would need ~ 12,000 microtubules pointing approximately in the right direction to overcome the viscous drag on the aster. This is thought to be unlikely[31]. This model also predicts that the speed of aster movement decreases as it moves away from the cortex where the sperm entered the egg. This is because the aster-size increases (and therefore its drag) but the compressive force that the pushing microtubules can sustain decreases (because their length increases). This is inconsistent with observations that sperm and telophase aster velocity is approximately constant throughout their movement [14, 19, 23]. By these arguments, the simple microtubule pushing model is probably unrealistic

B) *Pushing with a stiffened microtubule meshwork*: despite the arguments in A), we think pushing models cannot be ruled out yet. It seems feasible that a stiffened microtubules meshwork might be able to transfer large pushing forces over long distances.

If rods are bundled together so tightly that sliding between them is blocked, the effective diameter of the new rod is proportional to the square root of the number

of microtubules (n) used. From formula 1 it follows that the Euler force F_e is then proportional to n^2. For differently connected microtubules, like in a meshwork, the Euler buckling formula no longer applies. When microtubles are embedded in an elastic network, e.g. of actin filaments, they no longer buckle as a single curve when compressed, but rather in a series of bends whose spacing depends on the properties of the network. This allows even a single microtubule to bear a much larger compressive load [3].

We do not know the structure of the sperm aster, and whether the microtubules within it are bundled, crosslinked, or embedded in a network of actin or intermeditate filaments. The hollow appearance of asters in immunofluorescence, discussed above, is inconsistent with the single microtubule pushing models in A), and perhaps consistent with a physical picture of asters as a cross-linked stiffened meshwork. We could imagine that a stiff aster blows up like a balloon inside the sphere of cytoplasm (Fig. 3 C). Soon after fertilization the sperm aster only touches one side of the cell boundary, so it naturally centers as it expands. As soon as the aster fills up the whole cell, forces are approximately equal, until the aster breaks down. In telophase one could therefore imagine two balloons inside one cell that blow up and center and repel each other at the same time. We posit this model to encourage discussion. We note that a very stiff aster should be spherical, but this is not what we observe, especially in telophase where the two asters seem to delineate a plane where they meet at the cell center (Fig. 2 D).

C) *Pulling from the cortex with limited attachment sites*: pulling on microtubules by cortical dynein is a well established mechanism for moving asters in *C. elegans* and budding yeast[4, 5, 7]. A problem with naive cortical pulling models is that they tend to de-center asters, not center them. As more microtubules are likely to hit the closer boundary than the one that is further away. A model where all microtubules that touch the cortex generate pulling forces causes movement of the aster towards the boundary[11].

Grill and Hyman proposed an elegant solution, that only a limited number of motors or anchoring sites exist on the cortex [6]. In this model, cortical motors are saturated with microtubules, so more net pulling force is generated on the side that faces away from the center (Fig. 3 B). Laser cutting experiments suggest that this model is a good description for the early cells (~ 45 µm) in *C. elegans*[5]and evidence from variance of pulling forces was consistent with limited motor numbers in that system[32]. Presumably persuaded by the *C. elegans* and yeast data, most students of the centering problem now seem to consider cortical pulling model the general solution, ad fission yeast cells the small length scale exception[10, 11]. In our opinion, however, cortical pulling models cannot explain sperm and telophase aster movement in amphibian eggs, because the asters start moving well before microtubule reach the opposite cortex (e.g. Fig. 2 A and D). In *Xenopus*, unlike in *C. elegans,* the sperm centrosome and its aster start moving towards the cell center shortly after fertilization, well before microtubles reach the opposite cortex in immunofluorescence views (Fig. 2 A and B). It is

very hard to imagine that any aster microtubules can extend ~ 1200 µm within less than 10 minutes. All the microtubules we visualize by (admittedly crude) immunofluorescence imaging appear to grow out as a fairly homogeneous front at the surface of the aster. We see no evidence for a subset of faster and longer microtubules, and know of no mechanism by which a subset could grow much faster than the bulk population. Our estimate of aster expansion rate in the egg (~30µm/min increase of aster diameter => ~15µm/min microtubules growth rate) is fairly similar to the measured single microtubule plus-end growth rate in interphase egg extracts (~15µm/min[33]).

Another experiment that strongly argues against pulling from the cortex was performed by Herlant and Brachet ~ 100 years ago. A frog egg was fertilized with multiple sperms. Each sperm triggered the growth of its own sperm aster. The asters centered relative to the cellular boundary but also relative to each other (Fig. 4 A). Therefore the asters had to move away from the cortex that they were touching towards cortex they were not touching. This behavior is inconsistent with pulling from the cortex as the main or only centering mechanism. We will discuss how asters notice each other further below.

D) *Pulling on the cytoplasm*: In this model, a molecular motor that is able to move towards the microtubules minus-end (presumably dynein) is distributed throughout the cytoplasm and attached to something e.g. ER, yolk, or other cytoskeletal polymers (Figure 3D)[31, 34]. The longer the microtubules, the more

motors it engages, leading to a length-dependent pulling force, and therefore an attractively simple centering mechanism. This is similar to the mechanism proposed by Hays and Salmon for centering chromosomes in metaphase spindles in insect spermatocytes[35]. In *C. elegans,* yolk particles are transported to the center of the aster in a dynein-dependent way[36]. The drag forces generated by this movement could generate the required force. But cytoskeletal components such as intermediate filaments or actin also seem plausible as motor-anchoring elements. How could such elements be elastic enough to be pulled on but at the same time allow the sperm aster to move through it? Perhaps dynamic structures could fulfill both requirements. A beautiful experiment performed in Sand Dollar embryos [34] is consistent with this model, and inconsistent with A to C above: Hamaguchi and Hiramoto incubated the fertilized egg in the microtubule depolymerizing drug colcemid, which is readily converted into an inactive derivative, lumicolcemid, by 360nm light. Illuminating parts of the embryo with UV light generated defined regions in which microtubule growth was allowed. The sperm aster moved to the center of these UV-treated regions, and followed the UV-treated regions when it was moved. This worked independent of whether or not the region contained any cell cortex. This model, which we currently favor, focuses attention on the question of the physical nature of the egg cytoplasm, which must somehow be solid enough to sustain pulling forces, but liquid enough to allow aster movement. A potential clue to how this is possible is the nature of the trail left in the cytoplasm as the sperm aster moves through it. This trail is easily visualized in light micrographs as a region of

disturbed cytoplasm that persists for many minutes. Perhaps centrosomes can somehow melt the cytoplasm in their immediate vicinity, which then re-solidifies as the move on, leaving behind a long-lasting imprint of their passage.

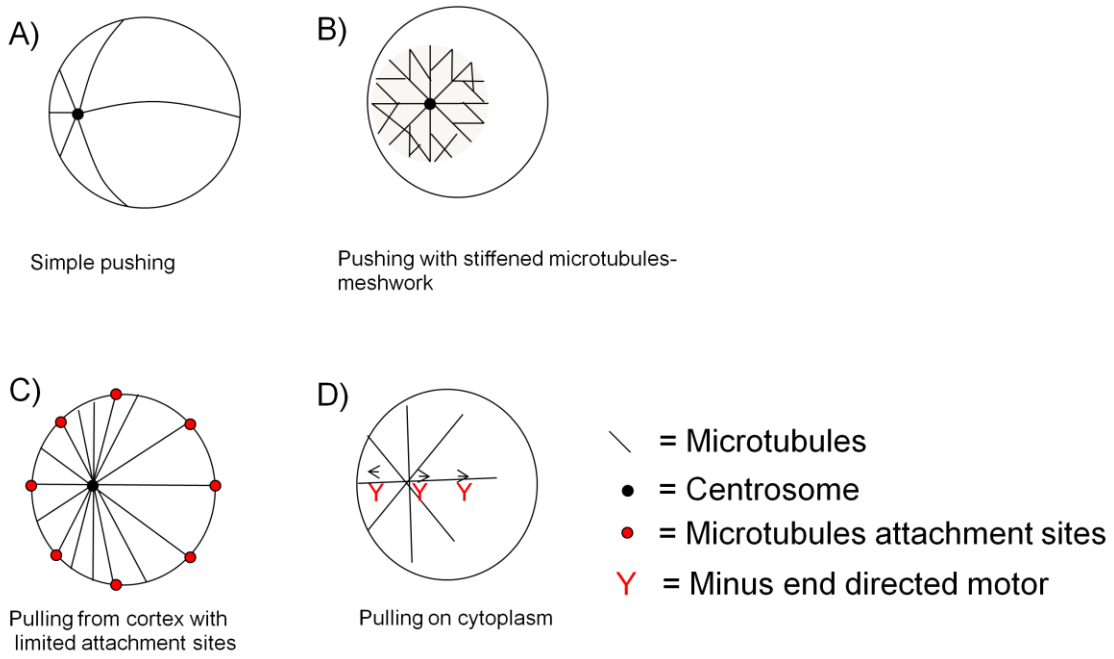

Figure III-3: Models on how asters could find the center of a very large cell. A) In the *simple pushing* model the force that can be transmitted via microtubules is inversely proportional to the square of their length.[30] B) In the *pushing with stiffened microtubules meshwork* model the aster is stiffened via bundling, crosslinking or embedding in an elastic gel [3]. Microtubules can transfer relevant pushing forces over long distance. C) In the *pulling on the cortex with limited attachment sites* model minus end directed motors are saturated with microtubules. The sum of forces on the centrosome points towards the cell's center.[6] D) In the *pulling on the cytoplasm* model minus-end directed motors are attached to a component of the cytoplasm (e.g. yolk or cytoskeleton). The longer a microtubule, the more motors are pulling which leads to centering.[31, 34]

How do asters interact with each other?

The behavior of multiple asters from a poly-spermic fertilization is interesting in its own right (Fig. 4 A) [37, 38] , and we think the way asters interact in this situation may also be relevant to normal telophase asters, where a pair of asters from the two spindle poles interact at the presumptive cleavage plane (Fig. 2 D). To allow comparison of these situations, we show an image of telophase asters at the end of the first mitosis in a dispermic embryo (Fig. 4 B). Likely similarity between the normal interaction of paired asters during telophase, and the abnormal interaction due to polyspermy, is evident from the similarity of all the aster boundaries. Microtubules from the different asters do not seem to inter-penetrate, rather they delineate a plane between interacting asters (which appears as a line in confocal micrographs) where the microtubule density is lower. Asters appear to treat this aster-aster boundary in a manner similar to the aster-cortex boundary, in that their centers move away from both kind of boundaries, to center in the space delineated by the combination of cell boundaries and aster-aster boundaries. Aster trajectories can be visualized in figure 4A by the trail that is left in the egg cytoplasm along the path followed by each centrosome towards the center of its own territory. This centering movement leads to rather precise spacing of asters in the polyspermic condition (Fig. 4A), and, we argue, directs the movement of the telophase asters away from each other in a straight line during normal telophase. The telophase aster-aster boundary is also of interest because initiates the cleavage furrow where it touches the cortex, as discussed

above. A century has passed since the regular spacing of polyspermic asters was described, and to our knowledge, the underlying mechanism is not understood. Based on modern understanding of microtubule organization, we propose three classes of model for discussion that are not mutually exclusive. The first two are related to mechanisms that have been discussed for formation of midzone and phragmoplast microtubule arrays during, respectively, animal and plant cytokinesis. However we note that midzones and phragmoplasts are probably based on anti-parallel bundles at the midline, while the aster-aster interaction is characterized by a lower density at the midline.

1) Multivalent, plus-end directed motors could push microtubules of opposing polarity apart (Fig. 4 C). This function is analogous to the proposed function of the MKLP1-RACGAP1 complex in animal cytokinesis[39], and it may be worth looking for those proteins, or others plus end directed cytokinesis mostors, between asters.

2) A physical barrier is assembled between two neighboring asters or within an aster (Fig. 4 D). For example, plus end-directed transport might lead to accumulation of vesicles between asters. This proposal is related to the telophase disc model for midzone organization during cytokinesis[40]. Consistent with it, a poorly defined physical structure of some kind, called the diastema, has

been observed between telophase asters in eggs[41, 42]. Dense accumulation of membranous organelles at plus ends of telophase microtubules was noted in a recent study of monopolar cytokinesis[43]. Concievable, a dense wall of vesicles could act as a physical barrier to microtubule polymerization, and direct aster movement as we discussed for the cortex in centring models B and D above.

3) Factors attached to astral microtubules (or to vesicles they accumulate) could depolymerize microtubules of opposite polarity, leading to the microtubule-free zone between asters (Fig. 4 E). This mechanism would not generate the kind of physical barrier required for aster centering by pushing models A and B above, but it would suffice to control microtubule length in such as way as to allow centering by model D. Support for this model might come from localization of known depolymerization factors such as Kinesin-8 and -13 depolymerases[44].

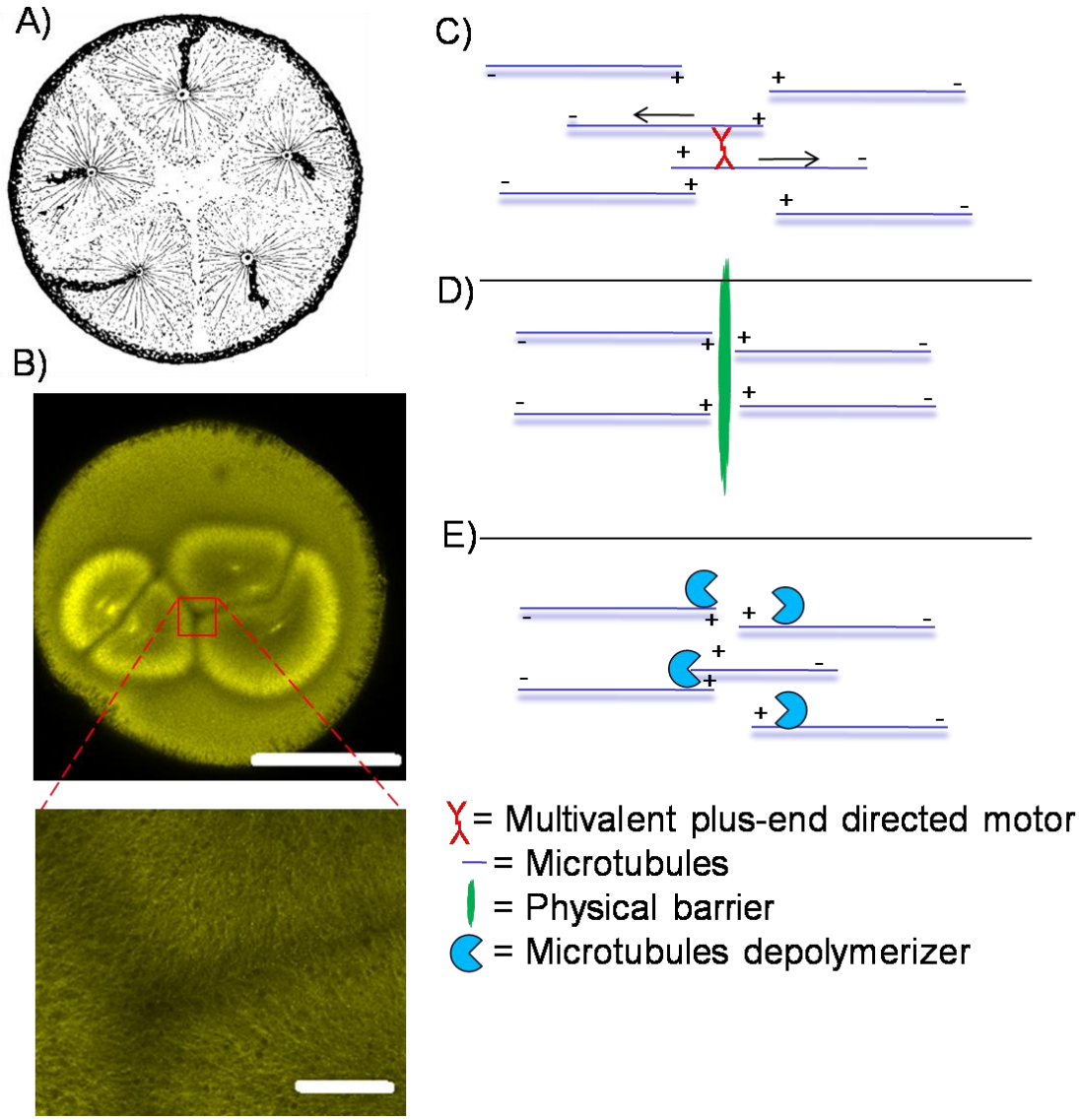

Figure III-4: How do asters notice each other? A) Sperm asters in polyspermic embryo space each other apart creating microtubule-sparse regions between them. Reprint by Herlant and Brachet (1910), kind permission of Springer Link.[37] B) Immunostaining of telophase in a di-spermic embryo with magnification of region between asters. Bars are 500 µm and 50 µm. C to E: Models that could explain how asters could notice each other: C) Multivalent plus-end directed motors push asters apart. D) A physical barrier is created between asters. E) Orientation-dependent microtubule depolymerizer chews up microtubules that enter with opposing polarity.

Conclusion

Studying how very large cells find their centers is interesting in its own right, and it also provides an original perspective on a universal problem. Because of their large sizes, amphibian eggs were among the first model organisms for cell division a century ago and earlier. These early studies have been largely forgotten in the modern obsession with molecular details and the difficulty of real-time imaging makes amphibian eggs challenging for modern methods. Nevertheless, it should be feasible to distinguish pushing versus pulling models for aster centering, for example using localized perturbation of microtubules dynamics[8]. Elucidating how asters sense, and repel, each other at their common boundaries may be more difficult. We suggest above some molecular candidates whose localization and function could be tested, and reconstitution of this phenomenon might be feasible in egg extracts. Physical extremes, in this case a very large cytoplasm, are always interesting in biology. Amphibian eggs, while challenging to work with, may provide insights that were missed in smaller, more transparent cells.

Materials and Methods

Immunostaining and handling of embryos was performed as described [23]. Dispermic embryo was obtained accidently.

Acknowledgment

We would like to thank Stefan Grill and Yifat Merbl for reading the manuscript, Will Ludington, Horatiu Fantana, Frank Jülicher, Jagesh Shah, Andrew Murray, Marc Kirschner, Cell division group Woods Hole and people in the Mitchison lab for helpful suggestions and discussion, Nikon Imaging Center (HMS) and Angela DePace for help with imaging. DJN was supported by the Life Sciences Research Foundation, sponsored by Novartis. This work was supported by the National Institutes of Health (NIH) grant GM39565

References

1. Mitchison TJ, Kirschner MW. Properties of the kinetochore in vitro. II. Microtubule capture and ATP-dependent translocation. J Cell Biol 1985; 101:766-77.

2. Tran PT, Marsh L, Doye V, Inoue S, Chang F. A mechanism for nuclear positioning in fission yeast based on microtubule pushing. J Cell Biol 2001; 153:397-411.

3. Brangwynne CP, MacKintosh FC, Kumar S, Geisse NA, Talbot J, Mahadevan L, Parker KK, Ingber DE, Weitz DA. Microtubules can bear enhanced compressive loads in living cells because of lateral reinforcement. J Cell Biol 2006; 173:733-41.

4. Grill SW, Gonczy P, Stelzer EH, Hyman AA. Polarity controls forces governing asymmetric spindle positioning in the Caenorhabditis elegans embryo. Nature 2001; 409:630-3.

5. Grill SW, Howard J, Schaffer E, Stelzer EH, Hyman AA. The distribution of active force generators controls mitotic spindle position. Science 2003; 301:518-21.

6. Grill SW, Hyman AA. Spindle positioning by cortical pulling forces. Dev Cell 2005; 8:461-5.

7. Adames NR, Cooper JA. Microtubule interactions with the cell cortex causing nuclear movements in Saccharomyces cerevisiae. J Cell Biol 2000; 149:863-74.

8. Burakov A, Nadezhdina E, Slepchenko B, Rodionov V. Centrosome positioning in interphase cells. J Cell Biol 2003; 162:963-9.

9. O'Connell CB, Wang YL. Mammalian spindle orientation and position respond to changes in cell shape in a dynein-dependent fashion. Mol Biol Cell 2000; 11:1765-74.

10. Vallee RB, Stehman SA. How dynein helps the cell find its center: a servomechanical model. Trends Cell Biol 2005; 15:288-94.

11. Dogterom M, Kerssemakers JW, Romet-Lemonne G, Janson ME. Force generation by dynamic microtubules. Curr Opin Cell Biol 2005; 17:67-74.

12. Montorzi M, Burgos MH, Falchuk KH. Xenopus laevis embryo development: arrest of epidermal cell differentiation by the chelating agent 1,10-phenanthroline. Mol Reprod Dev 2000; 55:75-82.

13. Elinson RP, Beckham Y. Development in frogs with large eggs and the origin of amniotes. Zoology 2002; 105:105-17.

14. Ubbels GA, Hara K, Koster CH, Kirschner MW. Evidence for a functional role of the cytoskeleton in determination of the dorsoventral axis in Xenopus laevis eggs. J Embryol Exp Morphol 1983; 77:15-37.

15. Hertwig O. Ueber den Werth der ersten Furchungszellen f ur die Organbildung des Embryo. Experimentelle Studien am Frosch- und Tritonei. Arch mikr Anat 1893; xlii:pp. 662-807.

16. Weber KL, Sokac AM, Berg JS, Cheney RE, Bement WM. A microtubule-binding myosin required for nuclear anchoring and spindle assembly. Nature 2004; 431:325-9.

17. Wong JL, Wessel GM. Defending the zygote: search for the ancestral animal block to polyspermy. Curr Top Dev Biol 2006; 72:1-151.

18. Felix MA, Antony C, Wright M, Maro B. Centrosome assembly in vitro: role of gamma-tubulin recruitment in Xenopus sperm aster formation. J Cell Biol 1994; 124:19-31.

19. Stewartsavage J, Grey RD. THE TEMPORAL AND SPATIAL RELATIONSHIPS BETWEEN CORTICAL CONTRACTION, SPERM TRAIL FORMATION, AND PRONUCLEAR MIGRATION IN FERTILIZED XENOPUS EGGS. Wilhelm Rouxs Archives of Developmental Biology 1982; 191:241-5.

20. Hausen P, Riebesell M. The early development of Xenopus laevis: an atlas of the histology. Springer-Verlag, 1991.

21. Reinsch S, Karsenti E. Movement of nuclei along microtubules in Xenopus egg extracts. Curr Biol 1997; 7:211-4.

22. Cha B, Cassimeris L, Gard DL. XMAP230 is required for normal spindle assembly in vivo and in vitro. J Cell Sci 1999; 112 (Pt 23):4337-46.

23. Wühr M, Chen Y, Dumont S, Groen AC, Needleman DJ, Salic A, Mitchison TJ. Evidence for an upper limit to mitotic spindle length. Curr Biol 2008; 18:1256-61.

24. Rappaport R. Experiments concerning the cleavage stimulus in sand dollar eggs. J Exp Zool 1961; 148:81-9.

25. Houliston E, Elinson RP. Patterns of microtubule polymerization relating to cortical rotation in Xenopus laevis eggs. Development 1991; 112:107-17.

26. Weaver C, Kimelman D. Move it or lose it: axis specification in Xenopus. Development 2004; 131:3491-9.

27. Houliston E, Elinson RP. Microtubules and cytoplasmic reorganization in the frog egg. Curr Top Dev Biol 1992; 26:53-70.

28. Gard DL, Cha BJ, Schroeder MM. Confocal immunofluorescence microscopy of microtubules, microtubule-associated proteins, and microtubule-organizing centers during amphibian oogenesis and early development. Curr Top Dev Biol 1995; 31:383-431.

29. Burbank KS, Groen AC, Perlman ZE, Fisher DS, Mitchison TJ. A new method reveals microtubule minus ends throughout the meiotic spindle. J Cell Biol 2006; 175:369-75.

30. Bjerknes M. Physical theory of the orientation of astral mitotic spindles. Science 1986; 234:1413-6.

31. Reinsch S, Gonczy P. Mechanisms of nuclear positioning. J Cell Sci 1998; 111 (Pt 16):2283-95.

32. Pecreaux J, Roper JC, Kruse K, Julicher F, Hyman AA, Grill SW, Howard J. Spindle oscillations during asymmetric cell division require a threshold number of active cortical force generators. Curr Biol 2006; 16:2111-22.

33. Tournebize R, Popov A, Kinoshita K, Ashford AJ, Rybina S, Pozniakovsky A, Mayer TU, Walczak CE, Karsenti E, Hyman AA. Control of microtubule dynamics by the antagonistic activities of XMAP215 and XKCM1 in Xenopus egg extracts. Nat Cell Biol 2000; 2:13-9.

34. Hamaguchi MS, Hiramoto Y. ANALYSIS OF THE ROLE OF ASTRAL RAYS IN PRONUCLEAR MIGRATION IN SAND DOLLAR EGGS BY THE COLCEMID-UV METHOD. Development Growth & Differentiation 1986; 28:143-56.

35. Hays TS, Wise D, Salmon ED. Traction force on a kinetochore at metaphase acts as a linear function of kinetochore fiber length. J Cell Biol 1982; 93:374-89.

36. Gonczy P, Pichler S, Kirkham M, Hyman AA. Cytoplasmic dynein is required for distinct aspects of MTOC positioning, including centrosome separation, in the one cell stage Caenorhabditis elegans embryo. J Cell Biol 1999; 147:135-50.

37. Brachet A. Experimental polyspermy as a means of analysis of fecundation. Arch Entwicklungsmech Org 1910; 30:261-303.

38. Herlant M. Recherches sur les oeufs di-et-trispermiques de grenouille. *Archs Biol* 1911; 26:103-328.

39. Glotzer M. The 3Ms of central spindle assembly: microtubules, motors and MAPs. Nat Rev Mol Cell Biol 2009; 10:9-20.

40. Andreassen PR, Palmer DK, Wener MH, Margolis RL. Telophase disc: a new mammalian mitotic organelle that bisects telophase cells with a possible function in cytokinesis. J Cell Sci 1991; 99 (Pt 3):523-34.

41. Selman GG. DETERMINATION OF THE 1ST 2 CLEAVAGE FURROWS IN DEVELOPING EGGS OF TRITURUS-ALPESTRIS COMPARED WITH OTHER FORMS. Development Growth & Differentiation 1982; 24:1-6.

42. Zotin AI. The Mechanism of Cleavage in Amphibian and Sturgeon Eggs. J Embryol Exp Morphol 1964; 12:247-62.

43. Hu CK, Coughlin M, Field CM, Mitchison TJ. Cell polarization during monopolar cytokinesis. J Cell Biol 2008; 181:195-202.

44. Howard J, Hyman AA. Microtubule polymerases and depolymerases. Curr Opin Cell Biol 2007; 19:31-5.

IV. Microtubule asters center in early embryo cells by dynein pulling from bulk cytoplasm

Martin Wühr[1,3,*], Edwin S. Tan[1], Jonathan Wong[2], H. William Detrich III[2], Timothy J. Mitchison[1,3]

[1]Department of Systems Biology, Harvard Medical School, [2]Department of Biology, Northeastern University, Boston, [3]Physiology Course 2008, MBL, Woods Hole, USA

* Correspondence: Martin.Wuehr@gmx.de

Relative contribution:

MW and TJM designed experiments and wrote manuscript. MW performed most experiments. ET synthesized Caged-Combretastatin. JW and WD helped making transgenic fish line.

Abstract

Hertwig showed in the 1880s that the cleavage plane tends to bisect the long axis of the cell, but how this works is unclear. We investigated this question in the very large cells of early frog and fish embryos, where spatial organizing mechanisms that operate in bulk cytoplasm are readily observed. We show that interphase asters center in these cells by dynein-mediated pulling forces. These forces act before astral microtubules contact the cortex they are moving toward, so dynein must pull from bulk cytoplasm, not the cell cortex as usually proposed. The cortex acts to limit microtubule length, which indirectly controls the strength of dynein-dependent pulling forces, and thus centers the aster in the cell. A microtubule exclusion zone that forms between sister asters also limits microtubule length, and thus promotes outward movement of sister asters. Astral microtubles are too short to directly position metaphase spindles in large embryo cells. Rather, spindle position is determined in the preceding interphase by astral microtubules. We present a model in which dynein pulling from bulk cytoplasm, operating in conjunction with microtubule-length limiting mechanisms, centers nascent spindles, and orients them along the long axis of the cell. This model explains cleavage plane geometry in early vertebrate embryos, and may apply more generally.

Results and Discussion

Astral rays of microtubules (asters) emanating from centrosomes are fundamental spatial organizers of cell division. In typical animal cells, paired asters at the spindle poles position and orient the metaphase spindle in the center of the cell, parallel to its longest axis[1, 2]. Despite their central role, the mechanisms by which asters center and orient spindles are still poorly understood. Proposed models for aster centering are system and scale specific: In very small cells like yeast, centering can occur via microtubules pushing against the cell cortex[3]. However, due to buckling of longer microtubules, this mechanism is unlikely to operate in larger cells. There, asters are thought to center by pulling forces on microtubules exerted by the minus end-directed motor cytolasmic dynein. Microtubules must sense the cortex in any centering mechanism, so it is natural to propose that dynein pulls from the cortex[2, 4, 5].

In millimeter-sized frog eggs, the sperm enters on the side, and its centrosome nucleates a huge sperm aster. This aster centers the male pronucleus, and captures the female pronucleus. The sperm aster starts moving to the cell center long before its microtubules contact the far cortex. In polyspermic amphibian embryos, multiple asters within a single cell space themselves out evenly relative to the cell cortex, but also relative to each other[6]. These classic observations are inconsistent with aster centering forces coming from dynein attached to the cortex (see previous paper[7] for a more complete argument.)

Aster movement in large embryo cells could be driven by pushing forces generated at the cortex[8] or by pulling forces generated in bulk cytoplasm[9]. These models can be distinguished by locally depolymerizing microtubules and following aster movement[9, 10], but this is difficult in amphibian embryos whose high yolk content precludes live imaging deep inside the cell. Early *Zebrafish* embryos also have large cells, and live imaging is feasible due to separation of yolk and cytoplasm. Tubulin immunofluorescence of fixed *Zebrafish* embryos revealed microtubules organization very similar to frog embryos[7, 11]. For live imaging we generated a transgenic *Zebrafish* line expressing the microtubule binding domain of ensconsin fused to three GFPs (EMTB-3GFP)[12, 13].

Zebrafish sperm enters the egg at a central location, and nucleates an aster that spans the whole cell (Fig 1A). This aster breaks down at mitosis onset, and the first mitotic spindle forms where the sperm aster deposited centrosomes and DNA (Fig. 1B). This spindle is small compared to cell size, and its astral microtubules are too short to reach the cortex, as in *Xenopus*. After anaphase onset, astral microtubules grow out dramatically from the separating sister centrosomes (Fig. 1 C). We will call these structures telophase asters. At the plane where the two telophase asters overlap, a zone of reduced microtubule density emerges by an unknown mechanism, that we will call the exclusion zone (Fig 1 C, D).

We believe the function of the exclusion zone is to limit the length of microtubules

that grow inwards between sister asters. As the sister asters expand, the centrosomes at their centers move apart, towards the center of the presumptive daughter cells (Fig 1, B, C, D. E). Centrosome separation movement starts long before the asters touch the cortex, so it cannot be driven by cortical dynein. Also before the asters touch the far cortex, the centrosomes duplicate, and the axis between them orients parallel to the longest axes of the asters (Fig 1. D). Interphase nucleii follow centrosomes in all cases (e.g. Fig. 1D), presumably by recruiting dynein to their surface[14]. Second mitotic spindles assemble between the separated centrosomes, around the time of cytokinesis (Fig 1 D,E). Again, their astral microtubules at metaphase are too short to reach the cortex. It takes until approximately cell cycle 5 in fish, and 8 in frog, for cells to become small enough that metaphase asters can touch the cortex (Wühr unpulished).

Live imaging in Zebrafish confirmed similarity of microtubule organization in early frog and fish embryos. In both systems centrosomes start moving towards the cortex before any microtubule touch that cortex, and they continue moving until microtubules pointing in opposite directions achieve equal lengths. Lengths are set on the cortex side by the cortex, and on the opposite side by the exclusion zone between asters. Metaphase asters are too short to reach the cortex, so both spindle position and orientation must be set by the preceding interphase asters. These similarities in frog and fish embryos allowed us to combine the technical advantages of each system to probe mechanisms of spatial organization in large cells.

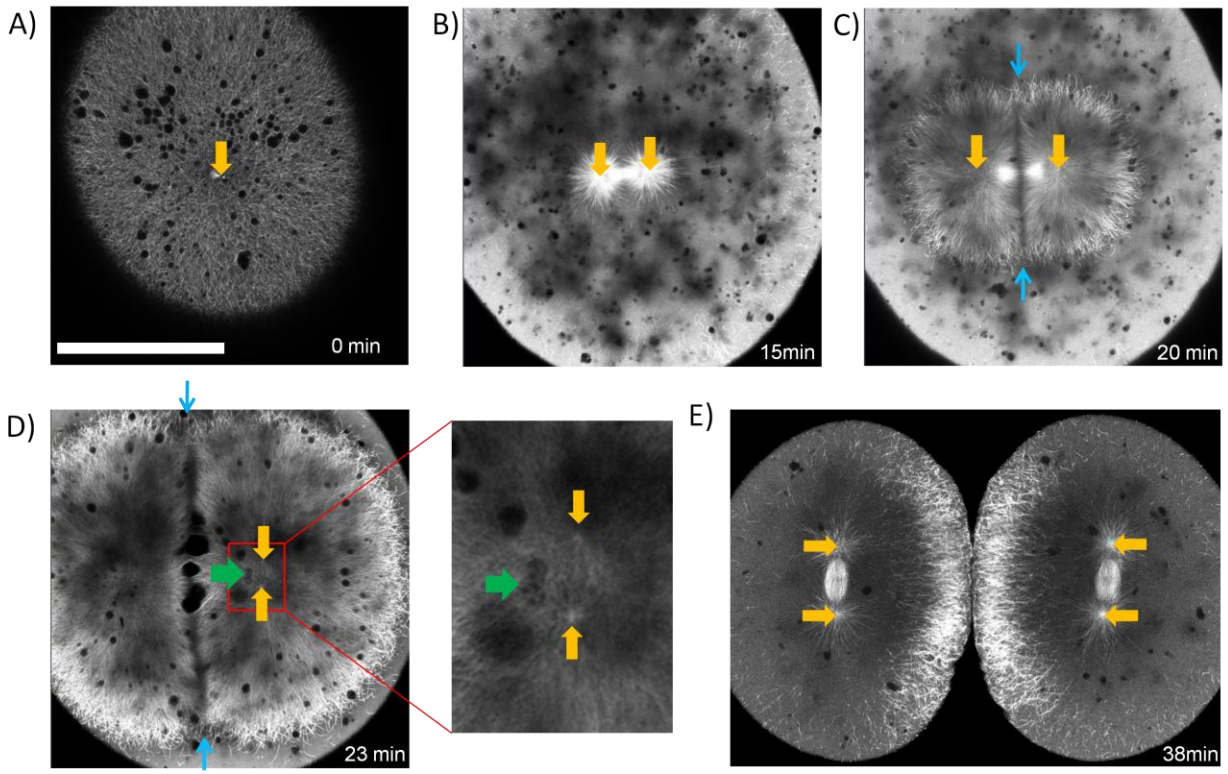

Figure IV-1: EMTB-3GFP transgenic zebrafish allows live imaging of microtubules organization in large cell. Orange arrows indicate positions of centrosomes A) Shortly after fertilization sperm aster covers cell B) Metaphase: Sperm aster breaks down and first mitotic spindle forms C) During anaphase-telophase astral microtubules grow out, and centrosomes move apart. Microtubule exclusion zones form in the plane where sister asters contact each other (between blue arrows). D) Centrosomes separated and align in the direction of the future spindle during late telophase (see enlargement). The centrosomes on the left are out of focus. Nuclei (green arrow) follow centrosomes, lagging behind. E) Second mitotic spindles assemble after cytokinesis (E is taken from different embryo). Bar = 200 µm

To determine if asters are positioned by pushing or pulling forces, we depolymerized microtubules in selected regions by uncaging a photo-activatable derivative of the microtubule depolymerizing drug Combretastatin 4A (Fig 2A). When the drug was activated with UV-light in defined regions close to asters (red area in Fig 2B), the asters started to disassemble preferentially on the irradiated side. As soon as an aster became anisotropic, its center moved away from the depolymerization zone. This observation argues strongly for aster postioning by

pulling forces. Movement induced by local depolymerization occurred before the remaining part of the aster touched the cortex, again arguing against a primary role for cortex-attached dynein. At the concentrations used (10μM) the drug in its caged form did not significantly interfere with microtubule dynamics (not shown), and similar irradiation of embryos without drug had no effect (n=3). We conclude that astral microtubules in zebrafish embryos exert pulling forces that are independent of aster-cortex contact.

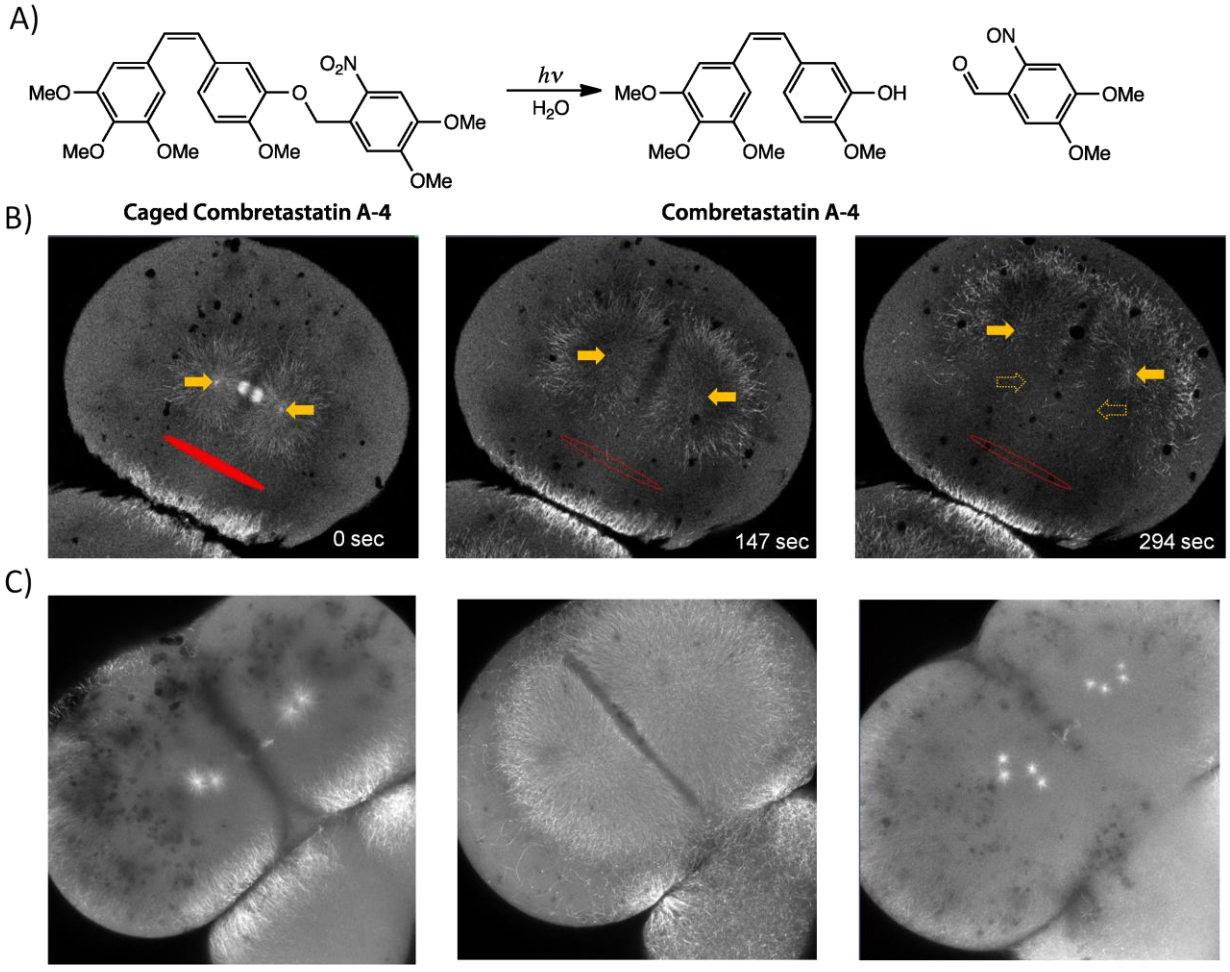

Figure IV-2: : Aster movement depends on dynein dependent pulling forces A) Structure of caged Combretastatin 4A; B) EMTB-3GFP embryos were incubated in caged-Combretastatin, and subjected to UV-irradiation in defined region (marked in red). Within

seconds, microtubule depolymerize selectively on the irradiated side. The remaining aster moved away from the irradiated region, arguing for pulling forces on asters. Full arrows mark position of centrosomes, hollow arrows on right mark original position. C) Injection of p150-CC1 blocks aster movement. Asters still grow out and break down under cell cycle control, but lose their ability to move or orient centrosomes.

The directionality of the pulling force suggests it is generated by a minus end-directed motor. Dynein is implicated in aster centering in other systems[15]. To inhibit dynein, we injected a dominant-negative fragment of the dynactin complex (p150-CC1) that binds to Dynein and blocks interaction with dynactin[16]. Interaction with Dynactin is required for most cellular activities of Dynein. We injected p150-CC1 into fish embryos shortly after fertilization. Aster growth was unperturbed; interphase asters still expanded to fill the cell, broke down in mitosis, and filled the cell again in the next telophase/interphase (Fig 2C). However, aster movement and centrosome orientation in telophase were completely blocked. As a result, multiple centrosomes accumulated in a small region, without organized orientation between sisters, and the asters they nucleated appeared to fuse. Thus aster movement, and probably also sister centrosome orientation, require dynein activity in Zebrafish embryos as they do in other systems[15]. We also tested for a role of Dynein in centering movement of the sperm aster in frog embryos. Eggs were injected with p150-CC1 shortly after fertilization, and fixed at times that in control cases we could observe the movement of the centrosome by the sperm-aster close to the center of the cell. By immunoflurescence, aster centering was severely inhibited (Suppl Fig. 1). We conclude that pulling forces on asters in frog and fish embryos depend on dynein-dynactin interaction, and thus that pulling force is most likely generated by dynein. Dynein must pull from sites dispersed throughout the cytoplasm to

explain how asters move long before their microtubules contact the cortex toward which they are moving.

We also investigated how spindles orient in large embryo cells. Metaphase asters are too small to sense cellular shape (Fig 1B, previously published[17]), and centrosomes are already aligned correctly before the nuclear envelope breaks down (Fig. 1D, 3A). They appear to align during telophase as the sister asters are moving apart. We previously hypothesized that the spindle axis is determined by asters in interphase/ telophase of the previous cell cycle[17]. These could be the sperm aster for mitosis one, and the sister telophase asters in subsequent mitoses. To test this idea, we imposed an artificial longest axis at the one cell stage of frog embryos by compressing them between glass plates[18], and asked when in the cell cycle the embryo positions its centrosomes relative to this imposed cell shape. Embryos were fixed in the compressed form at time points during the first cell cycle. By immunofluorescence staining of α-tubulin and γ-tubulin we distinguished cell cycle stages into prophase (before nuclear envelope break down), metaphase, anaphase/telophase and cytokinesis (Fig 3B). For each fixed embryo we measured the orientation of sister centrosomes relative to the longest axis of the cell (Fig 3C). Already in prophase, before mitotic spindle assembly, orientation of centrosomes relative to the longest cell axis differed only by an average of 4.9°± 2.4 SD (compare to random orientation of 45°). This orientation did not improve significantly in metaphase (4.2° ± 3.7, p=0.5, Student's t-test). Between anaphase and cytokinesis alignment improved significantly (p=0.001), presumably because the expanding telophase asters

begin to sense cellular shape. Cleavage planes were oriented with an average of 86.1° ± 2.8 relative to the artificial longest axis, showing that cleavage planes accurately respect the artificial centrosome orientation imposed before mitosis. We conclude that in frog embryos the sperm aster or telophase aster of the previous cycle senses cellular shape and converts the information into appropriate centrosome orientation at prophase. The prophase centrosome-centrosome axis then defines the metaphase spindle axis. This orientation depends on dynein but not on aster-cortex contact. Below, we argue that dynein pulling from bulk cytoplasm could orient centrosomes, as well as center asters.

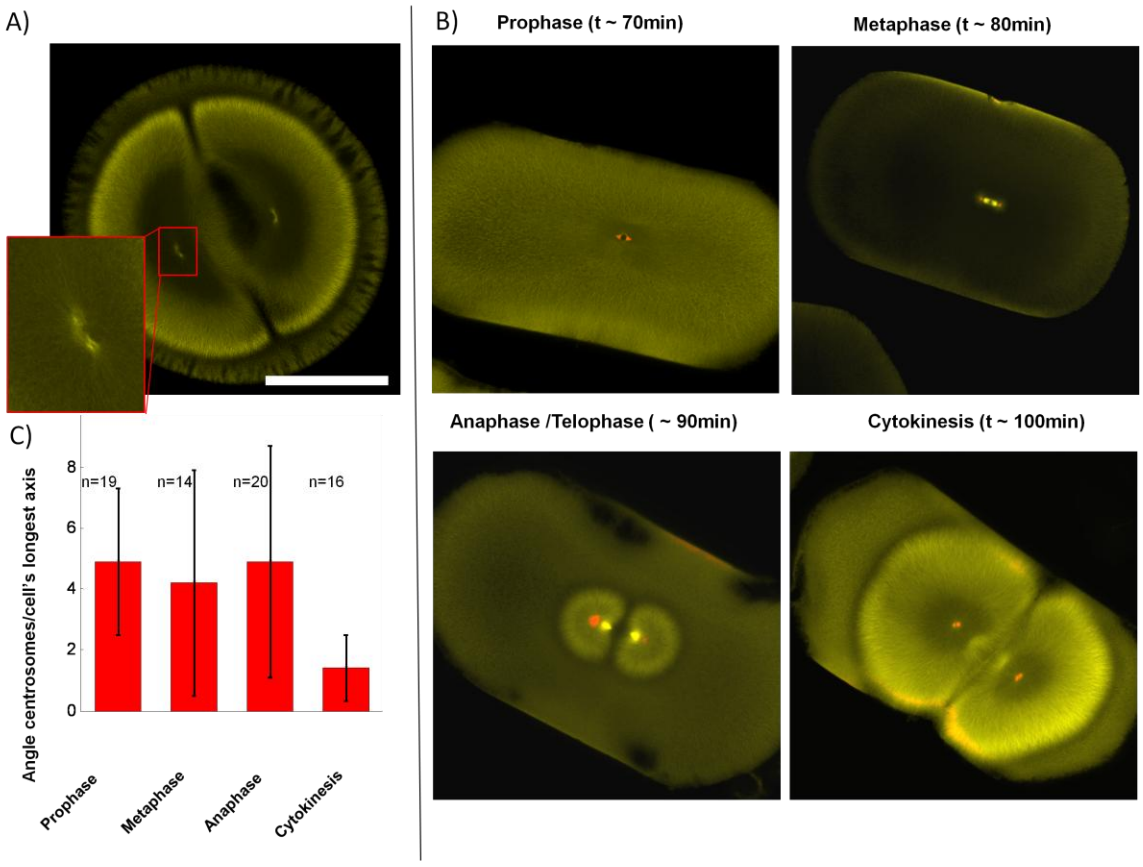

Figure IV-3: Spindles are positioned by asters prior to mitosis onset A) Tubulin immunofluorescence in frog embryo at anaphase-telophase of 1st mitosis, before

cytokinesis. Duplicated centrosomes are already aligned parallel to the longest axes of the daughter cells. Bar = 500 µm B) Frog embryos were artificially elongated by compression and fixed at different time points. Immunofluorescence against alpha-(yellow) and gamma-tubulin (red) allows scoring of centrosome orientation and cell cycle stage. Note centrosomes are already aligned in prophase, before nuclear envelope breakdown. D) Quantification of average centrosome orientation relative to longest cell axis (Angle measured between 0° and 90°, random orientation would be 45°) Centrosomes are already well aligned (4.9 °± 2.4 SD) before nuclear envelope breaks down, as soon as they can be visualized with gamma-tubulin staining. Alignment does not improve significantly towards metaphase (4.2 °± 3.7) or anaphase/telophase (4.9 °± 3.8). Alignment improves significantly once the expanding telophase asters touch the cortex, just before cytokinesis (1.4 °± 1.1)

In summary, we have shown that in very large vertebrate embryo cells, movement of asters to the center of the cell depends on dynein-dependent pulling forces on microtubles, but not on microtubule-cortex contact in the direction of aster movement. In telophase, sister asters interact to define a plane between themselves that excludes microtubules, and thus limits microtubule length. We have also shown that metaphase spindles are oriented by forces that position centrosomes before nuclear envelope breakdown. At this stage astral microtubules are long and can sense the cortex, and also the exclusion zone between asters. To explain all these findings, we propose a simple tug-of-war mechanism, where dynein anchored throughout cytoplasm engages astral microtubules, resulting in length dependent pulling forces (Fig. 4A inset). Microtubule length is limited by interaction of plus ends with the cortex, or with the exclusion zone between asters, and this is how the system senses cell shape, and the position of other asters. In frog, the sperm aster initiates on one side of the egg. Microtubules grow longer towards the cell center than towards the nearest cortex, because the cortex limits microtubule length. This results in imbalananced pulling force from dynein that moves the centrosome towards the cell center. However, the strongest stress on the centrosomes is perpendicular to

this movement direction. Microtubules are long in this axis, and there is little centrosome movement to relieve this stress generated by dynein's activity (Fig 4B). This stress causes strain in the aster that separates and orients sister centrosomes in prophase. As mitosis proceeds, and the sperm aster breaks down, the location and orientation of the sister centrosomes determine the location and orientation of the first mitotic spindle, which is small (~60 μm) relative to the egg (~1200 μm) (Fig 4C). At anaphase, kinetochore fibers pull sister chromatids a maximum of ~100μm microns apart. This distance is small compared to the cell, but sufficient to move sister a DNA molecule into the attraction spheres of the sister asters. Once the nuclear envelope reforms, nucleii follow asters using dynein on their surfaces (Fig 4,D)[14]. Microtubules that grow outwards in sister asters are unimpeded until they eventually reach the cortex. Microtubules that grow inward become length-limited by the exclusion zone. This results in a length imbalance, and dynein-mediated outwards movement of the asters. Lengths only balance when centrosomes reach a point midway between the cortex and the exclusion zone, i.e. the centers of the presumptive daughter cells. As for sperm movement, while net force during anaphase-telophase points outwards, the strongest stress in the system is perpendicular to this movement, (Fig 4C) resulting in centrosome orientation along the longest axis of the asters. In frog and fish, yolk is more concentrated towards the vegetal side of the embryo. This breaks the radial symmetry of both sperm and telophase asters in the plane normal to aster movement. It provides a third length limitation, to microtubules that grow downwards. This effect further controls aster shape

(shorter parallel to the Animal-Vegetal axis than normal to it) so that the first and second mitotic spindles orient horizontal, as well as normal to the direction of sperm movement (1st mitosis) or to the exclusion zone (subsequent mitoses). Cytokinetic furrows cleave where asters overlap[19], i.e. in the plane of the exclusion zone, using molecular mechanisms that are now partly elucidated[20]. This model explains aster centering, sister nucleus segregation in large cells, and cleavage plane orientation. It also explains how the first cleavage plane cuts through the sperm entry point[21]. The same model applies to fish embryos with the modification that the sperm in fish enters the top of the egg at the center[22].

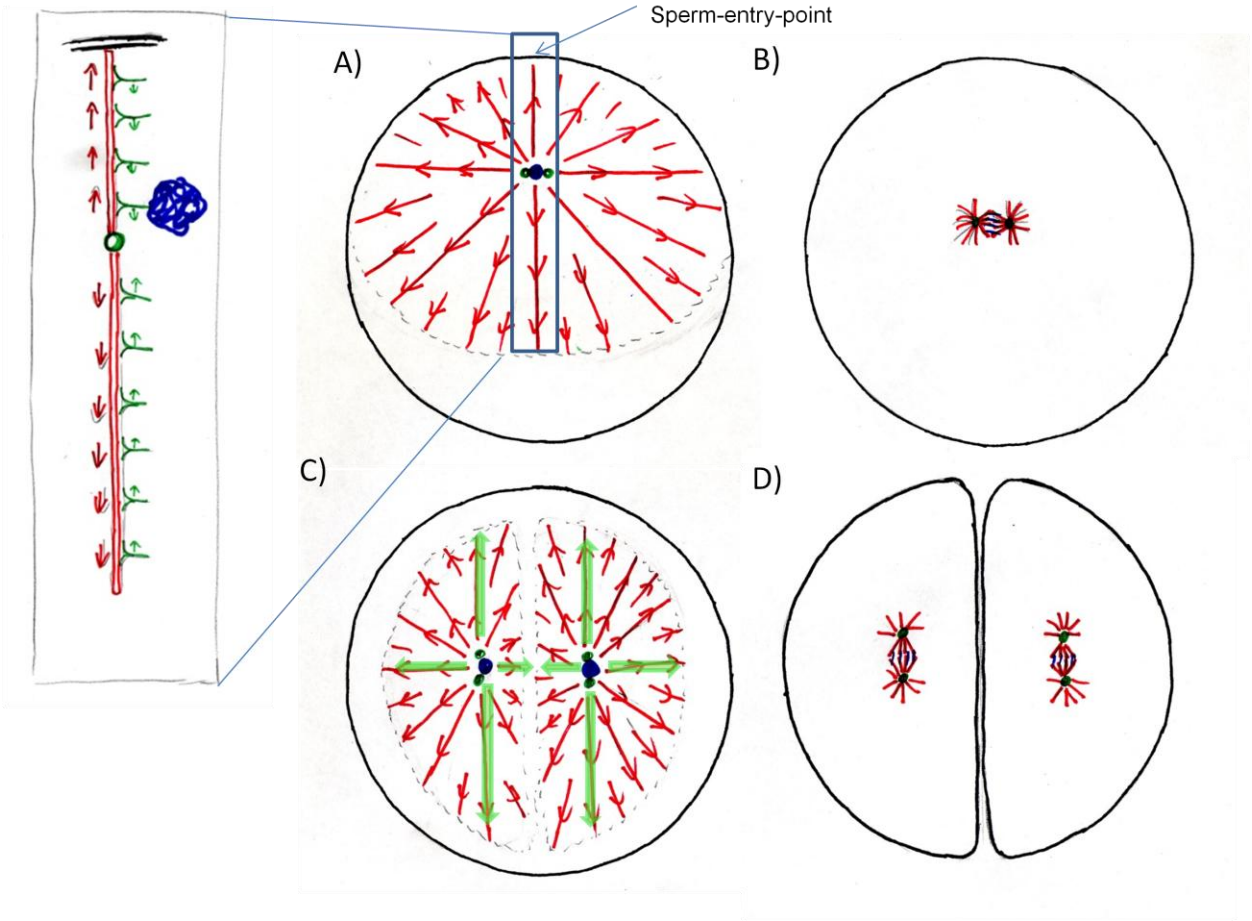

Figure IV-4: Astral Microtubules (red) pull with Dynein (green) on Cytoplasm to determine center and longest axis for cell division (DNA in blue). A) Sperm enters at periphery. Cellular boundary lead to asymmetry in sperm aster . Numbers of dynein (green) bound is proportional to microtubules length resulting in net force on centrosome towards cell's center. Sperm –aster is asymetric. Net force points to center of cell but strongest stress on duplicated centrosomes is perpendicular to movement. B) Sperm aster breaks down small first mitotic spindle forms. D) At onset of anaphase asters expand but do not grow into each other. The microtubules free zone between them generates the asymmetry in the aster leading to a net force on the centrosomes towards the future centers of the daughter cells. Centrosomes have already separated and are oriented along the longest axis of the asters . Centrosomes experience a net force in the directions of their movement but the largest stress on centrosomes is perpendicular to this movement (green arrows represent forces). E) The cytokinetic furrow divided the cell into two where the telophase asters overlapped cutting through the sperm-enty -point. Asters break down, small mitotic spindles form at center and along longest axis of daughter cells.

The Dutch biologist Swammerdam was probably the first person ever to note cell division, around 1665, when he observed the two cell stage of a fertilized frog

egg[23, 24]. The first cleavage stages in fish were first described in the early 19th century[25]. Hertwig first showed cleavage planes can be oriented by cell shape, so as to bisect the cells long axis. For the first time we can posit a unified model for cleavage plane determination, that depends on dynein pulling from bulk cytoplasm, and microtubule length limitation by the cortex and by aster-aster interactions. Our model finds strong support in very large cells, but it might apply more generally, to any system where asters or spindles center by pulling forces. In *C. elegans* , movement of the spindle to an off-center position depends on G-proteins that attach dynein to the cortex[26], but these G-proteins are dispensable for initial centering of the sperm aster during interphase-prophase[27]. Dynein is required for both movements[15]. We suggest dynein anchors in bulk cytoplasm to promote aster centering by a tug-of-war mechanism, and to specialized cortical sites to promote off-centering during asymmetric divisions and cell polarization. Further testing of our model will require elucidation of molecular mechanisms that anchor active dynein in bulk cytoplasm, and that limit microtubule length at the cortex and exclusion zones.

Materials and Methods

Imaging zebrafish:

EMTB-3GFP zebrafish line was generatet as described [28, 29]. Shortly after fertilization zebrafish embryos were mounted with help of an agarose mould in 0.1 x MMR (10mM NaCl; 0.2 mM KCl; 0.1 mM $MgCl_2$; 0.2 mM $CaCl_2$; 0.5 mM

HEPES, pH 7.5). and imaged with an upright or inverted Zeiss LSM 710 with 20x lense. Centrosome position could be derived by origin of microtubules.

Caged Combretastatin

O-[4,5-dimethoxy-2-nitrobenzyl]-2-methoxy-5-[(Z)-2-(3,4,5 trimethoxyphenyl)ethenyl]phenol. To a solution of combretastatin A4 (4 mg, 0.013 mmol) in DMF (1.5 ml) was added 4,5-$(MeO)_2$-2-NO_2-benzyl bromide (10.5 mg, 0.038 mmol), and Cs_2CO_3 (12.4 mg, 0.038 mmol). After stirring at room temperature for 22 hrs, the reaction mixture was diluted with dichloromethane. The organic layer was washed with water and brine, dried over $MgSO_4$, filtered, and concentrated under reduced pressure. The crude mixture was purified via flash SiO_2 column chromatography [EtOAc/hexanes (20%/80% to 25%/75%)] to give the desired compound with some impurities as a yellow solid (9.9mg, 96% yield). ^{1}H NMR (400 MHz, chloroform-*d*) δ 7.47 (s, 1H), 7.18 (s, 1H), 7.05 (s, 1H), 6.94 (dd, *J*=2.0 and 8.2 Hz, 1H), 6.92 (d, *J*=1.6 Hz, 1H), 6.82 (d, *J*=8.6 Hz, 1H), 6.48 (s, 2H), 6.45 (d, *J*=2.7 Hz, 1H), 4.01 (s, 3H), 3.97 (s, 3H), 3.88 (s, 3H), 3.82 (s, 3H), 3.68 (s, 6H).

Zebrafish embryos were mounted in 10 µM Caged Combretastatin. The drug was activated with a 405 Laser on a LSM 710 at 100% Laserpower. It took ~5 seconds to scan desired region with used scanning speed.

Dynein inhibition

P150-CC1 was expressed and purified as described previously[30] and dialyzed in XB +150mM Sucrose (10 mM HEPES, pH 7.7 1 mM MgCl2 0.1 mM CaCl2 100 mM KCl, 200mM Sucrose) and flash frozen (25mg/ml). Zebrafish were injected shortly after fertilization with ~4nl of protein solution and prepared for imaging as described above.

Xenopus embryos were fertilized at (~16°C). Shortly thereafter embryos were injected with ~25nl of p150-CC1 solution. Embryos were fixed 60 and 90 minutes after fertilization and prepared for immunofluorescence against α-tubulin and γ-tubulin as described [17]. Because the number of embryos that can be injected after fertilization is limited uninjected embryos served as control for fixation and immunostaining. Later embryos from same parents were injected with ~25nl of dialyzes buffer of p150-CC1, these embryos showed normal cleavage pattern.

Squishing Xenopus embryos.

Embryos were fertilized at room temperature, dejellied and squished between two glass plates. The glas plates were pressed together with a spring, the distance set by short pieces of wire (0.8mm diameter). Embryos were fixed in squished form with 90% MeOH 10% (H_2O, 0.5M EGTA). Immunofluorescence was performed as described [17].

Acknowledgment

The authors would like to thank Chi-Bin Chien for Tol2-kit plasmids, Chloe Bulinski for EMTB-3GFP plasmid and Trina Schroer for p150-CC1 plasmid, Nick Obholzer, Ramil Noche, people in the Mitchison lab for helpful suggestions and discussion, Will Ludington for help developing the squishing assay, Sandra Parker, Sean Megason and Angela De Pace for significant time on their microscopes. This work was supported by the National Institutes of Health (NIH) grant GM39565. H.W.D. was supported by NSF grant ANT-0635470.

References

1. Bjerknes, M. Physical theory of the orientation of astral mitotic spindles. *Science* **234**, 1413-1416 (1986).
2. Grill, S.W. & Hyman, A.A. Spindle positioning by cortical pulling forces. *Dev Cell* **8**, 461-465 (2005).
3. Tran, P.T., Marsh, L., Doye, V., Inoue, S. & Chang, F. A mechanism for nuclear positioning in fission yeast based on microtubule pushing. *J Cell Biol* **153**, 397-411 (2001).
4. Dogterom, M., Kerssemakers, J.W., Romet-Lemonne, G. & Janson, M.E. Force generation by dynamic microtubules. *Curr Opin Cell Biol* **17**, 67-74 (2005).
5. Kunda, P. & Baum, B. The actin cytoskeleton in spindle assembly and positioning. *Trends Cell Biol* **19**, 174-179 (2009).
6. Herlant, M. Recherches sur les oeufs di-et-trispermiques de grenouille. *Archs Biol* **26**, 103-328 (1911).
7. Wühr, M., Dumont, S., Groen, A.C., Needleman, D.J. & Mitchison, T.J. How does a millimeter-sized cell find its center? *Cell Cycle* **8**, 1115-1121 (2009).
8. Morgan, T.H. *Experimental embryology*. ((Columbia Univ. Press), 1927).
9. Hamaguchi, M.S. & Hiramoto, Y. Analysis of the role of astral rays in pronuclear migration in sand dollar eggs by the colcemid-UV method. *Development Growth & Differentiation* **28**, 143-156 (1986).
10. Burakov, A., Nadezhdina, E., Slepchenko, B. & Rodionov, V. Centrosome positioning in interphase cells. *J Cell Biol* **162**, 963-969 (2003).

11. Yabe, T. *et al.* The maternal-effect gene cellular island encodes aurora B kinase and is essential for furrow formation in the early zebrafish embryo. *PLoS Genet* **5**, e1000518 (2009).

12. Faire, K. *et al.* E-MAP-115 (ensconsin) associates dynamically with microtubules in vivo and is not a physiological modulator of microtubule dynamics. *J Cell Sci* **112 (Pt 23)**, 4243-4255 (1999).

13. von Dassow, G., Verbrugghe, K.J., Miller, A.L., Sider, J.R. & Bement, W.M. Action at a distance during cytokinesis. *J Cell Biol* **187**, 831-845 (2009).

14. Reinsch, S. & Karsenti, E. Movement of nuclei along microtubules in Xenopus egg extracts. *Curr Biol* **7**, 211-214 (1997).

15. Gonczy, P., Pichler, S., Kirkham, M. & Hyman, A.A. Cytoplasmic dynein is required for distinct aspects of MTOC positioning, including centrosome separation, in the one cell stage Caenorhabditis elegans embryo. *J Cell Biol* **147**, 135-150 (1999).

16. Quintyne, N.J. *et al.* Dynactin is required for microtubule anchoring at centrosomes. *J Cell Biol* **147**, 321-334 (1999).

17. Wühr, M. *et al.* Evidence for an upper limit to mitotic spindle length. *Curr Biol* **18**, 1256-1261 (2008).

18. Hertwig, O. Ueber den Werth der ersten Furchungszellen fuer die Organbildung des Embryo. Experimentelle Studien am Frosch- und Tritonei. *Arch. mikr. Anat.* **xlii**, pp. 662-807 (1893).

19. Rappaport, R. Experiments concerning the cleavage stimulus in sand dollar eggs. *J Exp Zool* **148**, 81-89 (1961).

20. von Dassow, G. Concurrent cues for cytokinetic furrow induction in animal cells. *Trends Cell Biol* **19**, 165-173 (2009).

21. Roux, W. Ueber die Ursachen der Bestimmung der Hauptrichtungen des Embryo im Froschei. *Anat. Anz.* **23** (1903).

22. Hart, N.H., Becker, K.A. & Wolenski, J.S. The sperm entry site during fertilization of the zebrafish egg: localization of actin. *Mol Reprod Dev* **32**, 217-228 (1992).

23. Swammerdam, J. Bibilia Naturae; sive historia insectorum, in classes certas redact **2** (1737).

24. Baker, J.R. Remarks on the discovery of cell-division. *Isis* **42**, 285-287 (1951).

25. Rusconi, D. Erwiederung auf einige kritische Bemerkungen des Herrn v. Baer ueber Rusconi's Entwicklungsgeschichte des Froscheis *Archiv Fuer Anatomie, Physiologie und Wissenschaftliche Medicin* (1836).

26. Grill, S.W., Howard, J., Schaffer, E., Stelzer, E.H. & Hyman, A.A. The distribution of active force generators controls mitotic spindle position. *Science* **301**, 518-521 (2003).

27. Kimura, A. & Onami, S. Local cortical pulling-force repression switches centrosomal centration and posterior displacement in C. elegans. *J Cell Biol* **179**, 1347-1354 (2007).

28. Kawakami, K. *et al.* A transposon-mediated gene trap approach identifies developmentally regulated genes in zebrafish. *Dev Cell* **7**, 133-144 (2004).

29. Urasaki, A., Morvan, G. & Kawakami, K. Functional dissection of the Tol2 transposable element identified the minimal cis-sequence and a highly repetitive sequence in the subterminal region essential for transposition. *Genetics* **174**, 639-649 (2006).

30. King, S.J., Brown, C.L., Maier, K.C., Quintyne, N.J. & Schroer, T.A. Analysis of the dynein-dynactin interaction in vitro and in vivo. *Mol Biol Cell* **14**, 5089-5097 (2003).

Supplementary Figure

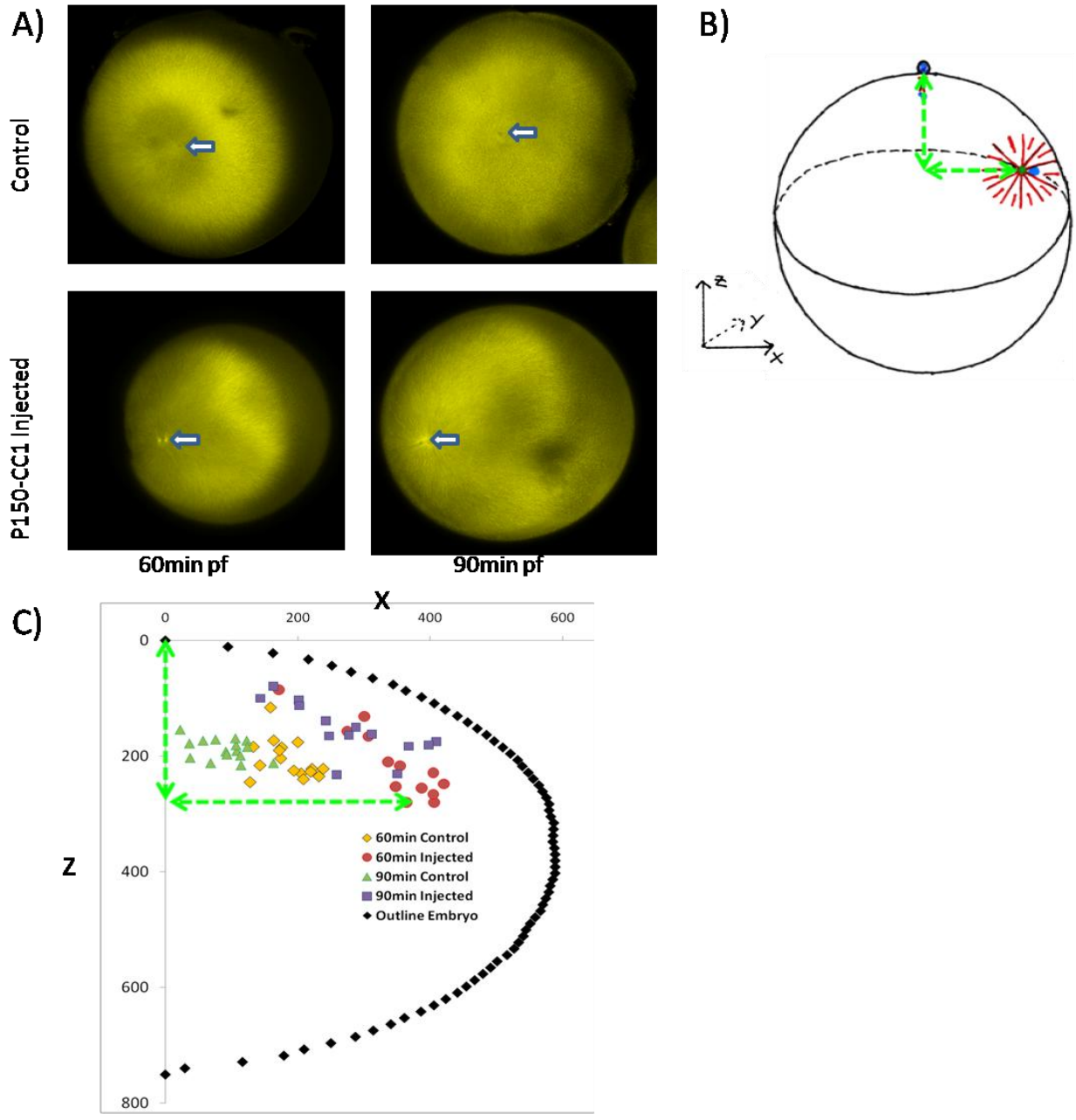

Suppl. Figure IV-1: Sperm-aster in frog embryos depends on dynactin to move centrosome: Embryos were synchroneously fertilized and fixed 60 and 90 min after fertilization. A) By staining against tubulin sperm aster formation and centrosome movement could be followed in p150-CC1 injected and control embryos. Arrow indicated position of centrosome. B) Because centrosome movement is three-dimensional, centrosome position was recorded relative to the embryo's axis of symmetry and the egg's top. C) Centrosome of injected and control embryos was plotted with circumference of embryos. In control embryos centrosomes move from the periphery towards the cell's center while p150-CC1 injected embryos centrosomes were located close to the cortex

V. Acknowledgement

I wanted to become a scientist since primary school age and it has been a long path since then. Thanks to my parents and especially my dad for his unwavering support. Having been an average pupil at best for most of my high school career, some excellent teachers nonetheless encouraged me to pursue a career in science. I especially thank Robert Veith, Mr. Förster, Arno Friese, Franz Mock, and Bene Bartl. Thanks to Andreas Woller, Klaus Westenthanner and Seppo Schmied for their support while getting through high school. I am deeply indebted to the supervisor of my Bachelor's thesis, Olaf Stemmann. During the six months in his lab I learned more about biology and how to do science than in the rest of my undergraduate education. Thanks to Titus Franzmann for his supervision during a rotation in the Master's program. Thanks to Christoffer Koch, especially for the encouragement to apply for the PhD program.

I had a great time working in the Mitchison lab. It is a very stimulating environment with a lot of very smart people, though nobody takes himself/herself too seriously and everybody is always willing to help. Special thanks to Aaron Groen, who taught me a lot about biochemistry. I am indebted to Dan Needleman and Sophie Dumont for taking me under their wings and introducing me to the more quantitative side of biology. Thanks to Chris Field for keeping the lab up and running, providing guidance on writing papers and this thesis, and always being available to help with anything. Whenever there was a finicky problem, Peg Coughlin was able to pull out one of her many amazing gadgets and most of the

time the problem was solved. Thanks to Edwin Tan for some chemical synthesis and especially for teaching me to do some on my own. Thanks to Joshua Reyes for a great rotation. Thanks for Kathy Buhl for help. Thanks to Philipp Niethammer, Bill Brieher, Puck Ohi, Guillaume Charras, Hao Yuan Kueh, Jue Shi, Katharina Ribbeck, Chi-Kuo Hu, James Orth, Nurhan Ozlu, Lino Huang, Yangzhong Tang, Sujeong Kim, Ethan Garner, Ani Nguyen, Kristin Krukenberg, and Miriam Ginzberg for their help and stimulating discussions. Thanks to Adrian Salic and Yao Chen, who started my initial project long before I joined the lab. Thanks to Bill Detrich and Johnathan Wong for their willingness to collaborate on a very risky project. Thanks to Nick Obholzer, Sean Megason, and Ramil Noche for introducing me to the zebrafish system. Also thanks to Sean Megason and Angela DePace for the extensive time on their microscopes.

Thanks to Mike Springer for the time he spent teaching me Matlab. Thanks to the MBL Cell Division Group, especially Tom Maresca and Jay Gatlin, for their willingness to share their experimental expertise and insight with me. Thanks to members of the MBL 2008 Physiology course, especially Will Ludington, Susanna Ribeiro, Horatiu Fantana, Martin Loose, and Katja Taute. Around the time of the Physiology course the main ideas for this thesis were developed. Tanks to my friends Benni Lehne, Yifat Merbl and Dann Huh for their support. Thanks to Samantha Reed for being such a wonderful organizer. Thanks to Rebecca Ward for reading manuscripts and being very supportive. Thanks to my DAC-committee members Dan Needleman, Jagesh Shah and Andrew Murray. Thanks to my PhD committee, David Burgess, Jagesh Shah, Marc Kirschner,

and David van Vactor for their time and effort. Thanks to my wonderful wife for all her support.

Most of all, thanks to Tim Mitchison. He is a great mentor with unsurpassed enthusiasm for science, who provided a nearly infinite amount of freedom but was always available for excellent advice and guidance.